Chemical Engineering Science 178 (2018) 118–135

Contents lists available at ScienceDirect

Chemical Engineering Science

journal homepage: www.elsevier.com/locate/ces

Synthesis of mass exchanger networks in a two-step hybrid optimization strategy

Michael Short [a], Adeniyi J. Isafiade [a,*], Lorenz T. Biegler [b], Zdravko Kravanja [c]

[a] Department of Chemical Engineering, University of Cape Town, Private Bag X3, Rondebosch, 7701 Cape Town, South Africa
[b] Department of Chemical Engineering, Carnegie-Mellon University, Pittsburgh, PA, USA
[c] Faculty of Chemistry and Chemical Engineering, University of Maribor, Slovenia

HIGHLIGHTS

- New technique for designing mass exchanger networks is proposed.
- Individual mass exchanger optimization is modelled in an NLP step.
- Detailed exchanger designs used to determine correction factors for MINLP step.
- Correction factors used to stir network optimization towards realistic designs.
- Solution obtained from detailed design is used to determine optimal network.

ARTICLE INFO

Article history:
Received 23 June 2017
Received in revised form 26 September 2017
Accepted 13 December 2017
Available online 14 December 2017

Keywords:
Mass exchanger networks
MEN
Non-linear programming
Mathematical programming
Orthogonal collocation
Packed columns

ABSTRACT

We present a new method for the synthesis of mass exchanger networks (MENs) involving packed columns. Simultaneous synthesis of MENs is typically done through the use of mixed-integer nonlinear program (MINLP) optimization, with simplifications made in the mathematical representations of the exchangers due to computational difficulty in solving large non-convex mixed-integer problems. The methodology proposed in this study makes use of the stage-wise based superstructure MINLP formulation for the network synthesis. This stage-wise superstructure model incorporates fixed mass transfer coefficients, fixed column diameters, no pressure drops, and unequal compositional mixing for models. In this paper, the simplified MINLP model is further improved by including a detailed individual packed column design in a non-linear programming (NLP) sub-optimization step, where orthogonal collocation is utilized for the partial differential equations, and optimal packing size, column diameter, column height, pressure drops, and fluid velocities. Detailed designs are then used to determine correction factors that update the simplified stage-wise superstructure models to more accurately portray the chosen design. Once the MINLP is updated with these correction factors, the model is re-run, with new correction factors obtained. This iterative procedure is repeated until convergence between the objective function of the MINLP and that of the NLP sub-optimization is achieved, or until a maximum number of iterations is reached. The methodology is applied to two examples and is shown to be robust and effective in generating new topologies, and in finding superior networks that are physically realizable.

1. Introduction

Decreasing the chemical industry's impact on the natural world and human health has been a key feature of the modern era of industrial development. In order to meet new emissions standards, decrease the threat of climate change, and reduce the impact of the chemical industry on human health and ecological systems, pollutant reduction is a necessity. In many cases, streams are required to be treated in order to discharge waste with acceptable levels of dangerous chemicals. Mass exchanger networks (MENs) are often employed to fulfil this task, using either other process streams or mass separating agents (MSAs) to absorb pollutants from streams to be discharged. Traditionally MENs have been designed with pinch technology, but these methods have the disadvantage that they are sequential in nature, with design targets being set and heuristics employed in order to find networks that approach or meet the targets. With the proliferation of the increased efficacy of non-linear and mixed-integer solvers, simultaneous optimization approaches have been shown to be more adept at finding

* Corresponding author.
E-mail address: Aj.isafiade@uct.ac.za (A.J. Isafiade).

https://doi.org/10.1016/j.ces.2017.12.019

Nomenclature

Abbreviations

HENS	heat exchanger network synthesis
IBMS	interval based MINLP superstructure
LMCD	logarithmic mean composition difference
MENS	mass exchanger network synthesis
MSA	mass separating agent
MINLP	mixed integer nonlinear program
NLP	nonlinear program
OCFE	orthogonal collocation on finite elements
SBS	supply-based superstructure
SWS	stage-wise superstructure
TAC	total annual cost

Sets

R	rich process streams
S	lean process and external streams
INT	superstructure intervals
K	composition locations

Indices

r	process rich streams
l	process lean and external lean streams
k	index representing interval, $1,\dots NOI$ and composition location, $1,\dots NOI+1$
ii	collocation point
jj	finite element
tt	total number of gridpoints over the entire height of the column

Parameters and variables

$ai_{r,l,k}$	packing specific surface area ($m^{-2}\ m^{-3}$)
$aiCor_{r,l,k}$	packing specific surface area correction factor
AC_l	annual operating cost per unit of lean stream l (\$/(g·y))
$AC_{ii,tt}$	parameters dependent on interpolating polynomial at ii collocation point and tt number of grid points
AF	annualisation factor
$Cl_{r,l,k,ii,jj}$	concentration of component in the lean stream in match r,l,k at collocation point ii and finite element jj (g/m^3)
$Cr_{r,l,k,ii,jj}$	concentration of component in the rich stream in match r,l,k at collocation point ii and finite element jj (g/m^3)
$D_{r,l,k}$	diameter of match r,l,k (m)
$Dcor_{r,l,k}$	diameter correction factor for match r,l,k
$Flux_{r,l,k,ii,jj}$	flux of component from rich stream to the lean stream in match r,l,k at collocation point ii and finite element jj ($g\ s^{-1}$)
$FloodPoint_{r,l,k}$	pressure drop at which flooding is likely to occur
FP	column packing factor
$Fr_{r,l,k}$	Froude number for match r,l,k
g	gravitational constant (ms^{-2})
G_r	flowrate of rich stream ($g\ s^{-1}$)
$Hcor_{r,l,k}$	Height correction factor for match r,l,k
He	Henry's law coefficient
$ky_{r,l,k}$	overall mass transfer coefficient for match r,l,k, ($g\ s^{-1}\ m^{-3}$)
$kya_{r,l,k}$	overall mass transfer coefficient multiplied by interfacial area ($g\ s^{-1}\ m^{-1}$)
$kyCor_{r,l,k}$	overall mass transfer coefficient correction factor for match r,l,k
L_c	upper bound for lean stream flowrate ($g\ s^{-1}$)
NC	number of collocation points
NE	number of finite elements
N_{total}	total mass flux over the element of packing dz
$PackCost_{r,l,k}$	the cost of packing (\$/m^3)
$PackFact_{r,l,k}$	packing factor (m^{-1})
$PackDens_{r,l,k}$	the density of the packing ($g\ m^{-3}$)
$Pdrop_{r,l,k}$	actual pressure drop (kPa/m)
$ReL_{r,l,k}$	Reynolds number for lean stream in match r,l,k
$ReR_{r,l,k}$	Reynolds number for rich stream in match r,l,k
$RHOL_{r,l,k}$	Lean stream density for match r,l,k ($g\ m^{-3}$)
$RHOG_{r,l,k}$	Rich stream density for match r,l,k ($g\ m^{-3}$)
$SA_{r,l,k}$	surface area of packing (m^2/m^3)
u	normalized spatial variable (defined in Eqs. (8) and (9))
Vis_r	viscosity of liquid stream l (Pa S)
$We_{r,l,k}$	Weber number for match r,l,k
X^s	supply composition of lean (process or external) stream
X^t	Target composition of lean (process or external) stream
Y_r^s	Supply composition of rich process stream
Y_r^t	target composition of rich process stream
Y_l^{*s}	equilibrium supply composition of lean (process or external) stream
Y_l^{*t}	equilibrium target composition of lean (process or external) stream
σ_c	critical surface tension
σ_l	surface tension of the liquid stream
$\Omega_{r,l}$	exchanged mass upper limit for match r,l,k
$\Phi_{r,l}$	driving force upper limit for match r,l,k
π	mathematical constant = 3.142
$\mu_{r,l,k}$	viscosity of the gas stream in match r,l,k (Pa s)
Sc	gas Schmidt number
ω	function of the wetted packed surface
a_G	experimental constant which is a function of packing
β	experimental constant which is a function of packing
ρ_r	density of the gas stream ($g\ m^{-3}$)
ρ_l	density of the liquid stream ($g\ m^{-3}$)
d_e	equivalent packing diameter (m)
$\in$	fractional voidage of the column packing
$G'_{r,l,k}$	superficial gas mass velocity in match r,l,k ($g\ m^{-2}\ s^{-1}$)
$L'_{r,l,k}$	superficial liquid mass velocity in match r,l,k ($g\ m^{-2}\ s^{-1}$)

Binary variable

$z_{r,l,k}$	represents the existence of match r,l in interval k in the optimal network

Positive variables

$A_{r,l,k}$	cross-sectional area of column r,l,k (m)
$dy_{r,l,k}$	mass exchanger driving force at rich end of exchanger
$dyrl_{r,l,k}$	mass exchanger driving force at lean end of exchanger
$fr_{r,l,k}$	Rich stream split branch flowrate for column r,l,k ($g\ s^{-1}$)
$fl_{r,l,k}$	Lean stream split branch flowrate for column r,l,k ($g\ s^{-1}$)
$G_{r,l,k}$	flowrate of rich stream in match r,l,k (m)
$H_{r,l,k}$	packed height for column r,l,k (m)
$h_{r,l,k,jj}$	height of individual finite element at finite element jj (m)
L_p	liquid flowrate at periphery of packing, $m^3\ s^{-1}\ m^{-1}$
L_l	flowrate of lean stream l ($g\ s^{-1}$)
$L_{r,l,k}$	flowrate of lean stream in match r,l,k (m)
$LMCD_{r,l,k}$	logarithmic mean composition difference between rich stream r and lean stream l in interval k
$M_{r,l,k}$	mass exchanged between rich stream r and lean stream l in interval k ($g\ s^{-1}$)
$y_{r,k}$	composition of rich process stream in composition interval boundary k
$x_{l,k}$	composition of lean (process or external) stream in composition interval boundary k

$x_{r,l,k,ii}$	Lean stream composition in match r, l, k at collocation point ii	$yr_{r,l,k}$	Rich streams' composition at the stream exit from the column
$y_{r,l,k,ii}$	Rich stream composition in match r, l, k collocation point ii	$yl^*_{r,l,k}$	Lean streams' composition at the stream exit from the column
$y^*_{l,k}$	equilibrium composition of lean (process or external) stream l in composition interval boundary k		

superior, and often counter-intuitive, solutions. Unfortunately, solver technology is still limited in its ability to guarantee globally optimal solutions for non-convex and mixed integer problems, meaning that large problems are difficult to solve and are often reformulated using simplified shortcut models to represent the individual exchangers. In so doing, the resulting network is often not physically attainable or the individual units are over- or under-designed. Examples of typical simplifications that have been employed include fixing diameters for all columns involved, simplifying capital costing equations, fixing column dimensions, ignoring pressure drops and flooding considerations, and fixing mass transfer coefficients for specific stream pairs.

This study presents a novel methodology for the synthesis of MENs. The approach first makes use of the same simplifications as previous authors at the network synthesis level, by formulating a mixed-integer nonlinear program (MINLP). The resulting network topology and mass balances are then used to form a non-linear program (NLP) optimization in a second step, whereby detailed packed column models are used to ensure that the designs are feasible with regard to packing and flooding/pressure drop considerations, variable mass transfer coefficients, and column diameters and heights. This solution is then used to obtain correction factors that are implemented back into a subsequent iteration of the MINLP. The novel methodology is applied to case studies that demonstrate that more realistic solutions for MENs are obtained as a result of the inclusion of detailed models, as well as in overcoming several further shortcomings associated with current methods.

The outline of the paper is as follows: Section 2 provides a literature review section that discusses mass exchanger network synthesis on one hand and packed column optimization on the other hand, Section 3 presents the methodology adopted which includes generation of correction factors, the non-linear programming step and the iterative procedure used for solution generation. Sections 4 and 5 present case studies and conclusions, respectively.

2. Literature review

2.1. Mass Exchanger Network Synthesis (MENS) and packed column optimization

The MENS problem was first defined by El-Halwagi and Manousiouthakis (1989) where the pinch approach for heat exchanger network synthesis (HENS) was extended to the application of mass exchange networks. Hallale and Fraser (2000a) extended the methods of El-Halwagi and Manousiouthakis (1989, 1990a, 1990b) to include capital costs targets and simplified column design methods. More detailed capital costing for both packed and staged columns were considered in subsequent papers (Hallale and Fraser, 2000a, 2000b, 2000c). These approaches, while effective, are sequential in nature and therefore fail to take into account all the variables involved in the design of a network. A simultaneous mathematical programming approach was first used by Papalexandri et al. (1994). Their study formulated the MENS problem as a mixed-integer nonlinear program (MINLP) where the network hyperstructure approach, developed by Ciric and Floudas, (1989) for HEN synthesis, was adapted for MENS. El-Halwagi (1997) notes that this approach excludes solutions by excluding certain configurations; it also excludes the designer from the design, and can potentially find only locally optimal solutions due to non-convex terms. Comeaux (2000) simplified the model formulation presented by Papalexandri et al. (1994), adopting pinch principles to formulate the MENS problem as an NLP of moderate size.

Most of the modern attempts at finding truly optimal solutions have been adapted from the stagewise superstructure (SWS) approach of HENS (Yee and Grossmann, 1990). In this approach a superstructure is constructed that attempts to embed the most probable network topologies. Szitkai et al. (2006) used a similar approach to Yee and Grossmann's (1990) approach to HENS in the synthesis of MENs. Their model was formulated as an MINLP and they presented a mostly linear single contaminant model as well as a multiple contaminant model with the addition of nonlinear constraints. Their model made the assumption that mixing streams must have the same compositions, limiting the solution space, but removing non-linearities. Emhamed et al. (2007) introduced a hybrid approach to MENS that combined both Hallale and Fraser's (2000a) super-targeting approach with the MINLP optimization strategy of Szitkai et al. (2006). Isafiade and Fraser (2008) presented a novel method of setting up superstructures in MENS, named the Interval-Based MINLP superstructure (IBMS) Model. The model defines the stages of the superstructure in terms of the supply and target compositions of the rich and lean streams. These authors found that the new method may provide better solutions than the model of Szitkai et al. (2006). The authors suggested that, by defining superstructure stages in this way, it is possible that the problem is more efficiently initialized and bounded, resulting in more efficient solution times (Isafiade & Fraser, 2008).

Azeez et al. (2012, 2013) extended the IBMS by exploring other possible interval-based options. Their study was extended to both HENS and MENS and defined the intervals by supply and target compositions in different ways, eventually resulting in the supply and target based superstructure, target and supply based superstructure, and the supply based superstructure (SBS) shown in Fig. 1.

Liu et al. (2013) used an NLP formulation to find optimal MENs with multiple components and used a genetic algorithm-simulated annealing algorithm hybrid approach. Their method does not rely on key components and uses the number of trays to account for capital costing. They present only a small example that fails to find the best solution, even with a simplified superstructure in their formulation (Liu et al., 2013).

Isafiade and Short (2016) extended the SBS model of Azeez et al. (2012) to include the diameter as a variable in the MINLP. They also included the overall mass transfer coefficient as a variable for each stream, by inclusion of Pratt's correlation (Leva, 1953) and by considering velocities of both rich and lean streams. These inclusions also allow us to consider the column's packing and flooding potential. Due to the highly non-linear nature of the additional equations, a specialized initialization strategy was proposed to get initial solutions. Once these were generated the resulting columns were checked for flooding. Different packings were selected for flooded columns and the model re-run. The model

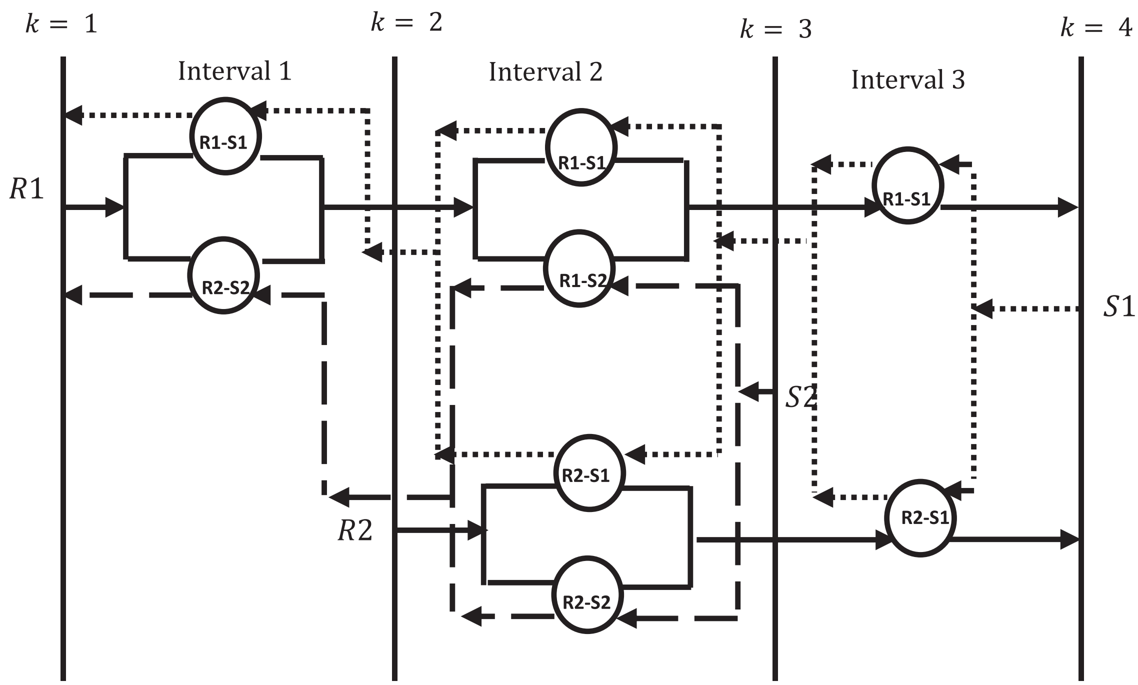

Fig. 1. Supply based superstructure (SBS) used in this paper, adapted from Azeez et al. (2012)

was successfully applied to both single and multi-period examples; however the highly nonlinear nature of the additional equations and the subsequent manual flooding check and change of packing parameters provided no guarantee of the globally optimal solution. Moreover, the model proved difficult to initialize and unrealistic columns were found with large diameters and small heights. As a result, this model is not used in the current study.

Much research has been done on the HENS problem in the last 20 years and many of the advances for MENS have indirectly come from the HENS research. For instance, Short et al. (2016a) made use of a novel method for the synthesis of HENs, whereby the initial network synthesis was achieved by an MINLP model similar to that of Yee and Grossmann's (1990) SWS. Noting that the SWS equations contain approximations of the heat exchanger areas, unrealistic fixing of heat transfer coefficients, lack of pressure drop considerations nor inclusion of multiple shells, the authors used more accurate heat exchanger heuristic models to design the network in detail. They found that the rigorously designed exchangers differed drastically from the MINLP shortcut model approximations. To help the MINLP find solutions that were more realistic, the authors included correction factors that forced the MINLP shortcut models to converge to the solution of the more rigorous design equations, with alternate solutions (iterations) between the MINLP model and rigorously designed versions of the MINLP model solutions. The resulting networks were thus physically attainable in a real design scenario and able to find new networks that used the detailed design information without including detailed design equations in the MINLP. In addition to this, the authors noted that during the iterative process many new designs were generated and the MINLP optimization solution was more likely to find globally optimal solutions over the course of the algorithm. The authors also extended the approach to multi-period HENS, showing the versatility and robustness of the approach (Short et al., 2016b). This study extends these results from the field of HENS to that of MENS; it includes correction factors (i.e., for diameter, column height, packing surface area, mass transfer coefficients) to the MINLP stage, followed by a more detailed NLP optimization of the individual packed columns, and using this information to update subsequent runs of the MINLP topology optimization. In this new formulation, the inclusion of detailed packed column optimization, as opposed to the heuristic, manual designs used in the study of Short et al. (2016a) for HENS, allow for more rigorously determined optimal designs for both the network and the individual columns.

Detailed packed column models include partial differential equations, a number of different approaches have been used in attempting to solve these equations. A popular method for solving partial differential equations in engineering is through the use of orthogonal collocation on finite elements (OCFE). It has been shown by various authors (Karacan et al., 1998; Biegler and Logsdon, 1989) that the use of OCFE can drastically decrease the CPU time needed and shows sufficient accuracy in approximating differential equations. In this study the individual unit optimization is done through an NLP optimization with orthogonal collocation on finite elements (OCFE) to represent the concentration profiles along the columns, novel costing models for selection of optimal packing, and constraints on column length to diameter ratios and flooding considerations. The solutions of these rigorous individual column models are then used to "guide" the model to the next MINLP iteration using correction factors, similar to the procedure utilized in Short et al. (2016a) for HENS. The methodology is described in detail in the next section.

3. Methodology

The methodology adapts the HENS methodology of Short et al. (2016a) to MENS along with rigorous individual mass exchanger optimization using NLP optimization. The MENS network topology optimization uses the SBS model of Azeez et al. (2013) because of its consistent performance across a number of examples, and its relative simplicity. The main adjustments made to the SBS model are presented below, with the rest of the model equations presented in Appendix A, with the principal addition in this study is the inclusion of correction factors. These correction factors, like those employed in Short et al. (2016a, 2016b), allow for the simplified models in the MINLP section to converge to the solutions obtained by the rigorous models used in the NLP sub-optimization. Moreover, a detailed objective function is shown in Eq. (1).

where $yr_{r,l,k}$ and $yl^*_{r,l,k}$ are the rich streams' and lean streams' compositions at the streams' exit from the column.

$$\min\left\{\begin{array}{l}\left[AF\left\{\sum_{r\epsilon R}\sum_{l\epsilon S}\sum_{k\epsilon K}\left(\begin{array}{l}[23,805\cdot(Dcor_{r,l,k}\cdot D_{r,l,k})^{0.57}\cdot 1,15\cdot Hcor_{r,l,k}\cdot H_{r,l,k}]+\\ \left[PackCost_{r,l,k}\cdot\frac{\pi}{4}\cdot(Dcor_{r,l,k}\cdot D_{r,l,k})^2\cdot Hcor_{r,l,k}\cdot H_{r,l,k}\right]\end{array}\right)\right\}\right]+\\ FC\left(\sum_{r\epsilon R}\sum_{l\epsilon S}\sum_{k\epsilon K}(z_{r,l,k})\right)+\left[\sum_{l\epsilon S}AC_l\cdot L_l\right]\end{array}\right\} \tag{1}$$

where AF is the annualisation factor, $D_{r,l,k}$ is the diameter of the column, $H_{r,l,k}$ is the packed height of the column, $z_{r,l,k}$ is the binary variable associated with the existence of a match, and FC is the fixed cost/installation cost of an exchanger. The first term in the first square bracket is related to the annualized variable capital cost of the exchangers, where the 23,805 value is related to the cost of the column shell, the value of 1.15 is to account for 15% inactive space in the column, thereby giving the true height of the column, as opposed to just the packed height. The second term, which includes the $PackCost_{r,l,k}$ variable, relates to the cost of the packing within the mass exchanger. AC_l is the cost of the lean streams or MSAs and L_l is the lean stream flowrate.

Correction factors are included in Eq. (2) below to calculate the overall mass transfer coefficient:

$$kya_{r,l,k} = ky_{r,l,k}.kyCor_{r,l,k}\cdot ai_{r,l,k}\cdot aiCor_{r,l,k} \qquad k\in K,\ l\in S,\ r\in R \tag{2}$$

where $ky_{r,l,k}$ is the initial overall mass transfer coefficient, which is later corrected by $kyCor_{r,l,k}$ between each iteration, $ai_{r,l,k}$ is the initial interfacial area of the packing which is later corrected by $aiCor_{r,l,k}$ between each iteration, and $kya_{r,l,k}$ is the combination of the two. Note that all of these are parameters in the MINLP, and they are updated only after the NLP run; they do not add to the complexity of the MINLP model.

Corrections factors are also used in the calculation of the height of each packed column $H_{r,l,k}$, as shown in Appendix A (Eq. (A12)). It should be noted that the height is calculated through the use of an approximation for the log mean composition difference (LMCD) (Szitkai et al., 2006; Azeez et al., 2012; Isafiade and Short, 2016). While the approximation (Equation (A11)) has favorable numerical properties (Shenoy and Fraser (2003)) it may still provide poor estimates of the LMCD under certain conditions.

Another difference between the original SBS model and the one in this study is the inclusion of unequal composition mixing. This was enabled by including Eqs. (3)–(6) in our model to obtain more accurate solutions and to allow for more interesting interplay between the NLP and MINLP subsections.

$$G_r = \sum_{l\in L} fr_{r,l,k} \qquad k\in K\ r\in R \tag{3}$$

$$L_l = \sum_{r\in R} fl_{r,l,k} \qquad k\in K\ l\in S \tag{4}$$

where $fr_{r,l,k}$ and $fl_{r,l,k}$ represent split flows for rich and lean streams respectively in the particular interval. The mass balances across each interval of the SBS are therefore also altered to include these new variables:

$$fr_{r,l,k}\times(y_{r,k}-yr_{r,l,k}) = M_{r,l,k} \qquad k\in K,\ l\in S,\ r\in R \tag{5}$$

$$fl_{r,l,k}\times(yl^*_{r,l,k}-y^*_{l,k+1}) = M_{r,l,k} \qquad k\in K,\ l\in S,\ r\in R \tag{6}$$

The remaining equations are shown in Appendix A (Eqs. (A1)–(A12) and the MINLP model can be writing as:

$$\text{Min Objective }(1),\quad \text{s.t.Equations }(3)-(6),\ (A1)-(A12). \tag{MINLP}$$

This MINLP model uses a mostly linear formulation that assumes many of the design parameters are constant for all columns; diameters, mass transfer coefficients, and packing characteristics, as well as the fact that pressure drops are not considered. It also uses other simplified equations that may result in columns that are wholly different when designed using detailed models. Even with all of the simplifications in the MINLP model, numerous authors have reported problems in finding globally optimal solutions. In addition, many authors have underlined the fact that it may be necessary to use specific initialization and bounding strategies in order to find suitable networks. Due to these issues we apply the more targeted approach in Short et al. (2016a). Once the solution to the MINLP is found, the resulting mass balances and exchanger matches are fed into the detailed unit design section.

Since much research deals with simulation of continuously contacting packed columns, any suitable method can be applied here. For example, the AspenPlus™, HYSYS, ChemSep™, or heuristic design approaches can be used as well as the detailed NLP optimization used in this study. On the other hand, since the literature on the deterministic optimization of packed column solvers is fairly sparse, a unique model is developed in the next section that allows for the packing characteristics to be solved along with other column specifics.

3.1. Non-linear programming step

The NLP model in this section allows for the simultaneous optimization of multiple columns in a network synthesis as well as for the determination of optimal packing sizes, diameters, heights, and flooding limitations through the use of detailed model equations. As with the MINLP model, isothermal columns are also used for the NLP. The NLP model is expanded to consider multiple columns with many variables, flooding considerations, packing characteristics with packing types fixed, and other design constraints. Moreover, temperature and detailed thermodynamics can be included through the use of a process simulator or another optimization model where fewer design considerations are taken into account. NLP optimization is further enabled through an easy implementation within a single optimization environment, such as GAMS (General Algebraic Modelling System) with reasonable solution speeds.

After the MINLP model solution is found, the solutions for the mass balances, flowrates, and compositions obtained are used to set up the optimization of the individual mass exchangers using detailed equations. The individual exchangers are optimized using a basic, general differential equation, where the mass flow, M, across a differential height element z is given by:

$$\frac{dM}{dz} = N_{total} \tag{7}$$

where N_{total} is the total mass flux over the element of packing. Since the MENS examples are typically non-reactive, contain single contaminants, and inert bulk streams, Eq. (7) will be sufficient if M is assumed to be the change in mass of the contaminant from the rich stream to the lean stream over the element dz. This is illustrated simply in Fig. 2.

Orthogonal collocation on finite elements (OCFE), employing Radau polynomials, is applied to solve this differential equation for each of the columns that result from the MINLP, with known boundary conditions for the differential equations at the ends of the exchangers. The height of each column is divided into a number of finite elements, with orthogonal collocation applied in each element. Also column height which is a variable is to be optimized in the NLP, the height of the column and therefore the height of each element is a variable. A graphical illustration of this technique

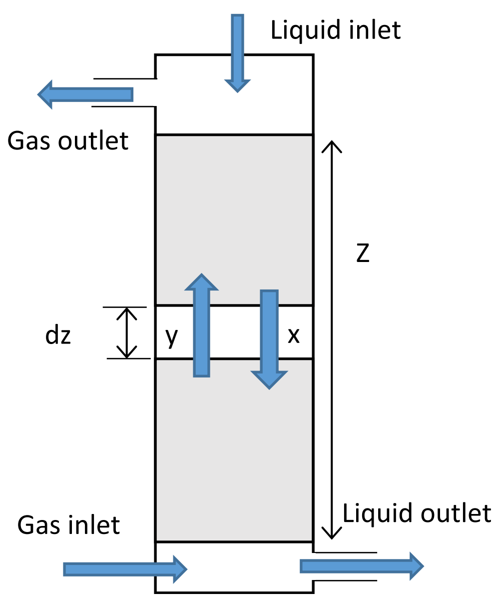

Fig. 2. Illustration of a packed column where Z is the height of packing.

is shown in Fig. 3 where the differential equation, $g(z)$, is split into jj finite elements of length h_{jj}. An interpolating polynomial, such as the Lagrange polynomial used in this study, is then applied on a number of collocation points within each of the elements.

Eq. (7) can be rewritten as:

$$\frac{L_{r,l,k}}{h_{r,l,k,jj}}\frac{dx_{r,l,k,tt}}{du} = Flux_{r,l,k,tt} \qquad k \in K,\ l \in S,\ r \in R,\ jj \in NE \tag{8}$$

$$\frac{G_{r,l,k}}{h_{r,l,k,jj}}\frac{dy_{r,l,k,tt}}{du} = Flux_{r,l,k,tt} \qquad k \in K,\ l \in S,\ r \in R,\ jj \in NE \tag{9}$$

where the subscripts r, l, k represent the individual match or exchanger from the MINLP section, and the subscript jj represent the finite elements where $jj \in 1, 2, \ldots, NE$. Subscript tt is the total number of gridpoints over the entire domain, i.e. $tt \in 1, 2, \ldots, (NE(NC-1)+1)$, NC is number of collocation points. $h_{r,l,k,jj}$ is the variable that determines the height of the individual finite elements (FEs). And for element e:

$$u = \frac{z - \sum_{jj=1}^{e-1} h_{r,l,k,jj}}{h_{r,l,k,e}} \qquad k \in K,\ l \in S,\ r \in R,\ jj \in NE \tag{10}$$

where

$$h_{r,l,k,e} = \sum_{jj=1}^{e} h_{r,l,k,jj} - \sum_{jj=1}^{e-1} h_{r,l,k,jj} \qquad k \in K,\ l \in S,\ r \in R,\ jj \in NE \tag{11}$$

When OCFE is applied we have:

$$\frac{L_{r,l,k}}{h_{r,l,k,jj}}\sum_{ii=1}^{NC} A_{ii,tt}x_{r,l,k,ii} = Flux_{r,l,k,tt} \qquad k \in K,\ l \in S,\ r \in R,\ jj \in NE,\ ii \in NC \tag{12}$$

$$\frac{G_{r,l,k}}{h_{r,l,k,jj}}\sum_{ii=1}^{NC} A_{ii,tt}y_{r,l,k,ii} = -Flux_{r,l,k,tt} \qquad k \in K,\ l \in S,\ r \in R,\ jj \in NE,\ ii \in NC \tag{13}$$

where $A_{ii,tt}$ is dependent on the interpolating polynomial, in our case, Lagrange polynomials. Subscript ii represents the collocation point, $ii \in 1, 2, \ldots, NC$.

In general, Radau collocation points are preferred as they allow for constraints to be set at the end of each element and give more efficient stabilization with high index differential algebraic equations (Biegler, 2007). Through the use of Radau collocation points, continuity can be maintained between elements easily with the

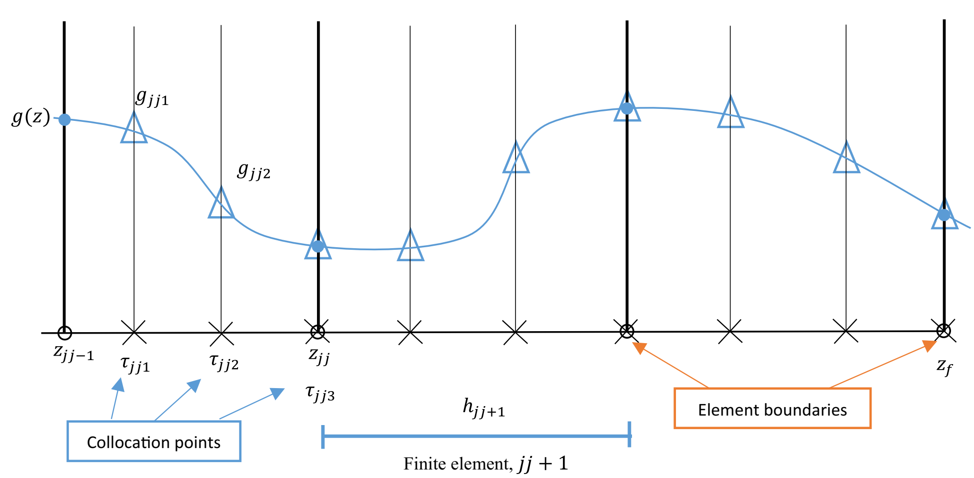

Fig. 3. graphical representation of collocation on finite elements. The triangles show dg/dz at collocation points and the circles show z at element boundaries, showing how continuity is retained.

last collocation point from the previous boundary providing the starting point for the next element. Radau collocation points are illustrated in Fig. 3. The boundary conditions for the first and last element for the supply and target concentrations for each column are provided from the MINLP.

The $Flux_{r,l,k,ii,jj}$ is related to the other variables in the model by the following relationship:

$$Flux_{r,l,k,ii,jj} = ky_{r,l,k} \cdot ai_{r,l,k} \cdot A_{r,l,k} \cdot (Cr_{r,l,k,ii,jj} - He \cdot Cl_{r,l,k,ii,jj}) \quad k \in K,\ l \in S,\ r \in R,\ jj \in NE,\ ii \in NC \tag{14}$$

where $ky_{r,l,k}$ is the mass transfer coefficient, $ai_{r,l,k}$ is the interfacial area of the packing, $A_{r,l,k}$ the internal area of the column, $Cr_{r,l,k,ii,jj}$ and $Cl_{r,l,k,ii,jj}$ are the rich and lean stream concentrations at collocation point, ii, and finite element, jj, respectively. He is the Henry's law coefficient and is the only parameter in this equation while all others are variables. If more rigorous thermodynamics are required and the isothermal assumption is removed, this should also be a variable related to the temperature. To determine the overall mass transfer coefficients in packed columns, numerous heuristic correlations have been proposed. Pratt's correlation (Leva, 1953) was the method used by Hallale and Fraser (2000b) and Isafiade and Short (2016), and has been used here to determine the overall mass transfer coefficient.

$$ky_{r,l,k} = \frac{G'_{r,l,k}}{\epsilon_{r,l,k}} \cdot a_G \cdot \left(\frac{de_{r,l,k} \cdot G'_{r,l,k}}{\epsilon_{r,l,k} \cdot \mu_{r,l,k}}\right)^{-0.25} \cdot Sc^{-0.667} \omega e^{\beta L_p} \quad k \in K,\ l \in S,\ r \in R \tag{15}$$

where $G'_{r,l,k}$ is the superficial velocity of the rich/gas stream, $\epsilon_{r,l,k}$ is the voidage of the selected packing, $de_{r,l,k}$ is the equivalent diameter of the packing, $\mu_{r,l,k}$ is the viscosity of the gas stream, a_G and β are experimental constants, L_p is the liquid flowrate at the periphery of the packing, ω is a function of the wetted packed surface, Sc is the Schmidt number. The term $\omega e^{\beta L_p}$ has been considered to be 1 to get an estimate of the mass transfer coefficient from the available experimental data, as in Hallale and Fraser (2000b) and Isafiade and Short (2016). Note that $ky_{r,l,k}$ is thus a function of the chosen packing's characteristics as well as the $G'_{r,l,k}$, which is a function of the column's diameter.

$$G_{r,l,k} = A_{r,l,k} \cdot G'_{r,l,k} \quad k \in K,\ l \in S,\ r \in R \tag{16}$$

$$L_{r,l,k} = A_{r,l,k} \cdot L'_{r,l,k} \quad k \in K,\ l \in S,\ r \in R \tag{17}$$

Eqs. (16) and (17) relate the volumetric flowrate of each stream in each match, $G_{r,l,k}$ for the gas/rich stream and $L_{r,l,k}$ for the liquid/lean stream, to the superficial velocities and the column areas. Note that the $G_{r,l,k}$ and $L_{r,l,k}$ are parameters obtained from the MINLP optimization, while the others are variables.

$$A_{r,l,k} = \frac{\pi}{4} \cdot (D_{r,l,k})^2 \quad k \in K,\ l \in S,\ r \in R \tag{18}$$

Eq. (18) simply relates the $A_{r,l,k}$ to the diameter of the column, $D_{r,l,k}$.

$$H_{r,l,k} \leqslant 25 * D_{r,l,k} \quad k \in K,\ l \in S,\ r \in R \tag{19}$$

$$H_{r,l,k} \geqslant 2 * D_{r,l,k} \quad k \in K,\ l \in S,\ r \in R \tag{20}$$

Eqs. (19) and (20) are limits suggested by Douglas (1988), which avoid short, but wide columns. These constraints were active in Example 1, but in Example 2, flowrate limits were removed so that large flowrates and low exchanger requirements yield feasible solutions with regard to flooding.

Similarly, there is a relationship between column diameter and packing size as follows:

$$15 * de_{r,l,k} \geqslant D_{r,l,k} \quad k \in K,\ l \in S,\ r \in R \tag{21}$$

In particular, for Raschig rings a ratio of upwards of 15 is preferred (Ibrahim, 2014). In order to avoid binary variables or disjunctive programming in the NLP optimization, discrete packing characteristic tables were fitted to curves (see Appendix B) so as to model packing characteristics as continuous variables with reasonable accuracy. This study consider Raschig rings with data taken from Perry's Chemical Engineering Handbook (Green and Perry, 2008) for Carbon Steel Raschig rings of various size.

$$PackFact_{r,l,k} = 2.0034 \cdot (de_{r,l,k})^{-1.564} \quad k \in K,\ l \in S,\ r \in R \tag{22}$$

$$SA_{r,l,k} = 5.0147 \cdot (de_{r,l,k})^{-0.978} \quad k \in K,\ l \in S,\ r \in R \tag{23}$$

$$\epsilon_{r,l,k} = 0.0569 \cdot \ln(de_{r,l,k}) + 0.9114 \quad k \in K,\ l \in S,\ r \in R \tag{24}$$

$$PackCost_{r,l,k} = 397431 \cdot (de_{r,l,k})^2 - 53449 \cdot (de_{r,l,k}) + 2366.1 \quad k \in K,\ l \in S,\ r \in R \tag{25}$$

where $PackFact_{r,l,k}$ is the packing factor (m^{-1}), $SA_{r,l,k}$ the surface area of the packing (m^2/m^3), and $PackCost_{r,l,k}$ is the cost of packing ($\$/m^3$), where, in the example it was updated from the year 1990 to the year 2000 using CEPCI indices. The year 2000 was chosen to allow for easier comparison with other authors, where the costing data for the examples were also sourced. In order to determine the interfacial area, $ai_{r,l,k}$, from the $SA_{r,l,k}$ of the packing, Eq. (26) from Onda et al. (1968) is used.

$$ai_{r,l,k} = SA^*_{r,l,k}\left(1 - \exp\left(-1.45 \cdot \left(\left(\frac{\sigma_c}{\sigma_l}\right)^{0.75} \cdot \left(\frac{\rho_l \cdot L'_{r,l,k}}{\mu_l \cdot SA_{r,l,k}}\right)^{0.1} \cdot (Fr_{r,l,k})^{-0.05} \cdot (We_{r,l,k})^{0.2}\right)\right)\right) \quad k \in K,\ l \in S,\ r \in R \tag{26}$$

This equation was verified by Mores et al. (2012) to be the most accurate prediction of $ai_{r,l,k}$ when compared with other empirical correlations. Here ρ_l is the density of the lean stream, σ_c is the critical surface tension of the packing and σ_l the surface tension of the liquid. $Fr_{r,l,k}$ is the Froude number:

$$Fr_{r,l,k} = \frac{SA_{r,l,k} \cdot (L'_{r,l,k})^2}{g} \quad k \in K,\ l \in S,\ r \in R \tag{27}$$

where g is the gravitational constant. $We_{r,l,k}$ is the Weber number:

$$We_{r,l,k} = \frac{\rho_l \cdot (L'_{r,l,k})^2}{SA_{r,l,k} * \sigma_l} \quad k \in K,\ l \in S,\ r \in R \tag{28}$$

The Reynolds' numbers of the lean and rich streams, represented by $ReL_{r,l,k}$ and $ReR_{r,l,k}$ respectively, are determined using Eqs. (29) and (30) below:

$$ReL_{r,l,k} = \frac{\rho_l \cdot L'_{r,l,k}}{\mu_l \cdot ai_{r,l,k}} \quad k \in K,\ l \in S,\ r \in R \tag{29}$$

$$ReR_{r,l,k} = \frac{\rho_r \cdot G'_{r,l,k}}{\mu_r \cdot ai_{r,l,k}} \quad k \in K,\ l \in S,\ r \in R \tag{30}$$

These Reynolds' numbers are used in the determination of the actual pressure drop across the column, $Pdrop_{r,l,k}$.

Finally, the most common method to determine the flooding in a packed column is through the use of the generalized pressure drop correlation (Sinnot, 2005). Isafiade and Short (2016) used this correlation in order to select different packings for packed columns in their model, however the selection was done outside of the optimization. For this study the method of Jamialahmadi et al. (2005)

was used in order to account for the pressure drop explicitly in the NLP:

$$Pdrop_{r,l,k} = 94\left(\frac{ReL_{r,l,k}^{1.11}}{ReG_{r,l,k}^{1.8}} + 4.4\right)6 \cdot \left(1 - \frac{\in_{r,l,k}}{de_{r,l,k} * \in_{r,l,k}^{3}}\right) \cdot \rho_r \cdot {G'_{r,l,k}}^2 \quad k \in K,\ l \in S,\ r \in R \tag{31}$$

The point at which flooding occurs can be calculated using the method of Kister and Gill (1991), converted to the appropriate units:

$$FloodPoint_{r,l,k} = \frac{249.089}{0.3048} * 0.12 * (0.3048 * PackFact_{r,l,k})^{0.7} \quad k \in K,\ l \in S,\ r \in R \tag{32}$$

with the following inequality constraint used to ensure that the optimal design has a pressure drop below the flooding point:

$$FloodPoint_{r,l,k} \geqslant Pdrop_{r,l,k} \qquad k \in K,\ l \in S,\ r \in R \tag{33}$$

Combining these equations leads to the NLP model given by:

$$\text{Min Objective (1)}, \quad \text{s.t.Equations (2)–(33), (A1)–(A12)} \qquad \text{(NLP)}$$

with all binary variables fixed to values determined in the previous MINLP problem. Problem (NLP) allows for the optimization of the individual packed columns obtained from the network generated in the MINLP by using more rigorous models. These rigorous models take into account many aspects that are not included in the MINLP, such as flooding considerations, column diameter, packing size, flux changes along the column, variations in the overall mass transfer coefficients, etc. The information obtained problem (NLP) can then be used to guide the MINLP to more accurate solutions based on these rigorous designs.

3.2. Correction factors and iterative procedure

After problem (MINLP) is solved and the resulting exchangers are rigorously optimized in problem (NLP) from the previous section, correction factors are determined in a manner similar to that of Short et al. (2016a). These correction factors are implemented in order to "guide" the shortcut models in the MINLP towards the solutions obtained in the NLP. Each correction factor is just factor applied to the current parameters and variables, as described in the subsequent paragraph and listed in Table 1.

In all other mathematical programming-based MENS approaches, apart from that of Isafiade and Short (2016), the diameter has been kept as a fixed parameter. As discussed previously, the approach of Isafiade and Short (2016) has numerous limitations, specifically in flooding and packing considerations and in the additional numerical complexity in the MINLP. This new approach maintains the diameter as a fixed parameter in the MINLP, but now allows for the parameter to be updated in subsequent iterations to resemble the diameter of rigorously optimized packed columns by updating the diameter via the $Dcor_{r,l,k}$ correction factor. It is calculated by dividing the diameter of the detailed packed column design obtained from the NLP by the fixed diameter in the MINLP. Similarly, the correction factors $kyCor_{r,l,k}$ and $aiCor_{r,l,k}$ are used to update the fixed $ky_{r,l,k}$ and $ai_{r,l,k}$ respectively in the MINLP to represent the more accurate $ky_{r,l,k}$ and $ai_{r,l,k}$ determined in the NLP.

Table 1
List and purpose of corrections used in the study.

Correction Factor	Purpose
$kyCor_{r,l,k}$	Correction for the overall mass transfer coefficient, $ky_{r,l,k}$
$aiCor_{r,l,k}$	Correction for the interfacial area of the packing, $ai_{r,l,k}$
$Hcor_{r,l,k}$	Correction to column height, $H_{r,l,k}$
$Dcor_{r,l,k}$	Correction for column diameter, $D_{r,l,k}$
$PackCost_{r,l,k}$	The updated packing cost obtained from the NLP step

The $PackCost_{r,l,k}$ correction is the cost determined from the NLP that is input for each individual "match" in the MINLP, as determined by the NLP. Notice that as with the other correction factors discussed thus far in this section, $PackCost_{r,l,k}$ is a variable in the NLP model but input as a parameter to the MINLP.

$Hcor_{r,l,k}$ is the only correction factor applied to a variable in the MINLP. This correction factor is used to correct the height, $H_{r,l,k}$, of the packed column in the MINLP to more accurately represent the actual column design in the NLP. In the MINLP the height is calculated using Eq. (A12) (Appendix A). This equation uses Chen's approximation of the log mean composition difference (Eq. (A11)), which has been shown by other authors to consistently underestimate the actual log mean composition difference, with large errors under certain conditions. A detailed comparison can be found in Shenoy and Fraser (2003) and Isafiade and Short (2016). Since problem (NLP) uses Eqs. (8) and (9) to represent the mass balance across the exchanger, the approximated $H_{r,l,k}$ in the MINLP is updated to represent this more accurately determined $H_{r,l,k}$ from the NLP.

As was the case in Short et al. (2016a), between each cycle the amount of change that a correction factor can undergo is limited. This ensures that the solution space is not too drastically altered between runs. In the case of the example presented in this study, the correction factors were limited to a change of no more than 5% between iterations. A flowchart that describes this algorithm is presented in Fig. 4.

3.3. Solution strategy

This section presents some of the methods used to ensure the model was robust enough to be automated, with special focus on the initialization strategy.

3.3.1. MINLP initialisation

When initializing the model it is important to have initialized parameters that underestimate the objective function in the MINLP step. This is done so that as the algorithm continues, no solutions are omitted (Short et al., 2016a; Short et al., 2016b). Parameter initialization for the MINLP are determined by first running the MINLP and NLP once (with estimated parameters) in order to obtain values that can be expected, and then using the values that are going to underestimate the objective function for all the parameters. For example, if the initial exploratory run gave $ky_{r,l,k}$ of 0.025, 0.03, 0.045, and 0.04 for the four exchangers, the initialization for all matches in the MINLP would be chosen as 0.05, as this would give an underestimation of the height and therefore objective function for all matches. Similar procedures were followed for the other parameters' initial values. The $Hcor_{r,l,k}$ initial value is 1, as this is only a correction to a variable that will be unknown.

3.3.2. NLP initialisation

Due to the size and non-convexity of the problem (NLP) a specific initialization strategy was required. The initialization strategy involved a succession of NLP subproblems, each one more complicated and non-linear than the next, with the preceding subproblem providing the initialization for the next. In doing this, a potentially feasible solution was provided as a starting point for the subsequent more complex model until the final model, presented above was able to be solved. This strategy proved effective in providing feasible solutions to all of the subproblems and through all of the iterations of the examples, thus providing evidence for its robustness and efficacy.

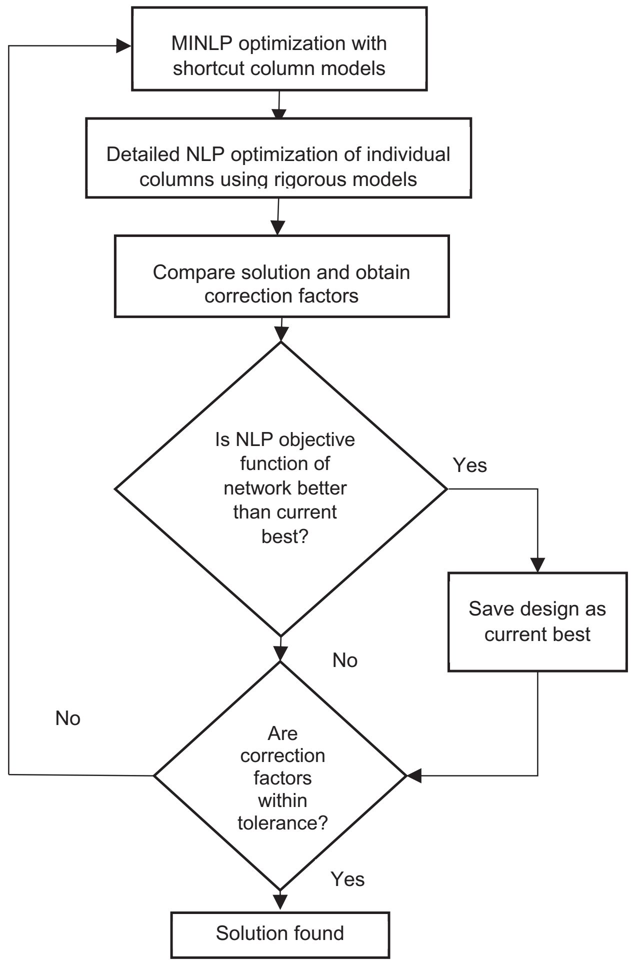

Fig. 4. Iterative procedure used in this study . adapted from Short et al. (2016a)

3.4. Solution Algorithm/Solvers

Problem (MINLP) is solved with DICOPT/GAMS with GAMS version 24.2.3 with CPLEX as the MILP solver, CONOPT as the NLP solver and DICOPT as the MINLP solver. The computer was equipped with an Intel Core™ i7-4700MQ 2.4 GHz CPU and 16 GB of RAM. The MINLP typically took between a few seconds to 4 min to solve, differing between successive iterations and examples based on the initialisations. Problem (NLP) makes use of CONOPT/GAMS and typically took less than a second to solve, however if the initialisation subproblems are included, the solutions of all subproblems could sometimes run for up to 4 min.

The algorithm itself is easy to implement and does not add complexity to either the MINLP or NLP as it iterates. The NLP formulation proved to be extremely robust, finding feasible solutions for almost any starting network provided by the MINLP. The MINLP, however still had numerous issues finding feasible solutions throughout the iterative procedure, as also reported by other authors. When initial points were changed as a result of the correction factors from a previous iteration, the MINLP would often become infeasible. Whenever the procedure was halted due to an infeasibility in the MINLP, the value associated with the Big-M formulation was changed until a feasible solution was found and then the iterative procedure was resumed from that point.

4. Case studies

The methodology was applied to two examples. The first is adapted from Isafiade and Short (2016), who originally adapted the problem from Hallale and Fraser (2000a, 2000b). The example comprises two rich streams and two lean streams. One of the lean streams is a process MSA, limited in available flowrate (with cost attached), while the other is a more expensive external MSA with unlimited available flowrate. The MEN should be designed in order to remove hydrogen sulphide from the two gas streams, R1 and R2. R1 is coke-oven gas and R2 is the tail gas from a Claus unit. The problem data associated with this example is included in Table 2, with additional information included in Table 3. The second example is adapted from Hallale (1998) and consists of 5 gaseous rich streams and 3 lean streams, demonstrating the model's effectiveness at handling larger problems. The rich streams consist of mostly air and contain the contaminant ammonia, while the 3 MSAs are all water-based, with 2 of them being process streams and 1 an external MSA. The problem data for this problem are shown in Tables 4 and 5. For all problems considered, carbon steel Raschig rings were the only random packings considered and thus $a_G = 0.123$ and $\sigma_c = 0.075$ for all examples (Green and Perry, 2008). The SBS method was used in setting up the MINLP superstructure.

4.1. Examples

4.1.1. Example 1

The initial values for the MINLP for Example 1, prior to any correction factors being implemented were $ai_{r,l,k} = 300$ m^2 m^{-3}, $ky_{r,l,k} = 0.05$ kg s^{-1} m^{-3}, $D_{r,l,k} = 0.35$ m, and $PackCost_{r,l,k} = 1000$\$m^{-3}. Problem (MINLP) contains 175 equations, 10 discrete variables, and 161 continuous variables, and Problem (NLP) contains 21,107 equations and 21,130 variables. During the course of the algorithm, 2 distinct topologies were found, with various minor differences in split flows and mass transferred in each exchanger. During iterations 1–17, a solution network containing the same 5 columns was found. This solution (at iteration 17) is shown in Fig. 5 with the detailed exchanger variables shown in Table 6. This 5-exchanger solution is very similar, in terms of exchanger mass duties, to the

Table 3
Other stream parameters used in Example 1.

Match	Density ($RHOG_{r,l}$) (kg m^{-3})	Viscosity ($\mu_{r,l}$) (Pa S)	Surface Tension (N·m^{-1})
Rich streams			
R_1, S_1	1.14	1.886×10^{-5}	0.0728
R_1, S_2	1.50	1.587×10^{-5}	0.0225
R_2, S_1	1.14	1.886×10^{-5}	0.0728
R_2, S_2	1.50	1.587×10^{-5}	0.0225
Lean streams			
S_1	900	0.0011	
S_2	842.5	0.0013	

Table 2
Stream data for Example 1. The *AF* was set to 0.2 and the FC = \$30,000. Sc = 0.7 for all liquid streams.

Rich streams	G (kg s^{-1})	Y^s	Y^t	MSAs	L_c (kg s^{-1})	m	X^s	X^t	Cost (\$yr^{-1})/(kg s^{-1})
R_1	0.9	0.0700	0.0003	S_1	2.3	1.45	0.0006	0.0310	117,360
R_2	0.1	0.0510	0.0001	S_2	∞	0.26	0.0002	0.0035	176,040

Table 4
Stream data for Example 2. The *AF* was set to 0.2 and the FC = $15,000. Sc = 0.7 for all liquid streams.

Rich streams	G (kg s^{-1})	Y^s	Y^t	MSAs	L_c (kg s^{-1})	m	X^s	X^t	Cost ($kg^{-1})
R_1	2.0	0.005	0.001	S_1	1.8	1.2	0.0017	0.0071	0
R_2	4.0	0.005	0.0025	S_2	1.0	1.0	0.0025	0.0085	0
R_3	3.5	0.011	0.0025	S_3	∞	0.5	0.0	0.017	0.001
R_4	1.5	0.010	0.005						
R_5	0.5	0.008	0.0025						

Table 5
Stream parameters for Example 2.

	Density ($RHOG_{r,l}$) (kg · m^{-3})	Viscosity ($\mu_{r,l}$) (Pa · s)	Surface Tension (N·m^{-1})
All Rich streams	1.14	1.886×10^{-5}	
All lean streams	1000	0.001	0.0728

solution of Isafiade and Short (2016). The solution at iteration 1 would therefore be the same solution as would be found without the addition of the correction factors or the iterative procedure. While the solutions are similar in terms of mass flows in each exchanger, the associated costs differ with the solution found in Isafiade and Short (2016) which had a TAC of 371,275$/y, while the rigorous solution presented here is 515,748$/y. This is due, in part, to the addition of an exchanger fixed cost in this study, which is not present in Isafiade and Short (2016). If the additional fixed costs are removed from the objective function in this study, it would yield a solution of 365,748$/y, even though the associated packing costs are higher in each of the exchangers than the packing used in Isafiade and Short (2016). This solution compares well to those of other authors and the current authors believe that this solution is a more accurate representation of the problem as the different sized packings' variable costs are considered, as well as a more accurate representation of the composition profiles along each column. This solution has been presented for comparison only, as the actual optimal solution was found after 27 iterations and had a different topology.

The optimal solution was found to be the network presented in Fig. 6 and Table 7 with 4 units and a TAC of 485,273$/y (365,273$/y if the fixed cost is removed). This network was found in the final iteration, after the MINLP and NLP solutions converged to within a percentage of each other, with very little change between the

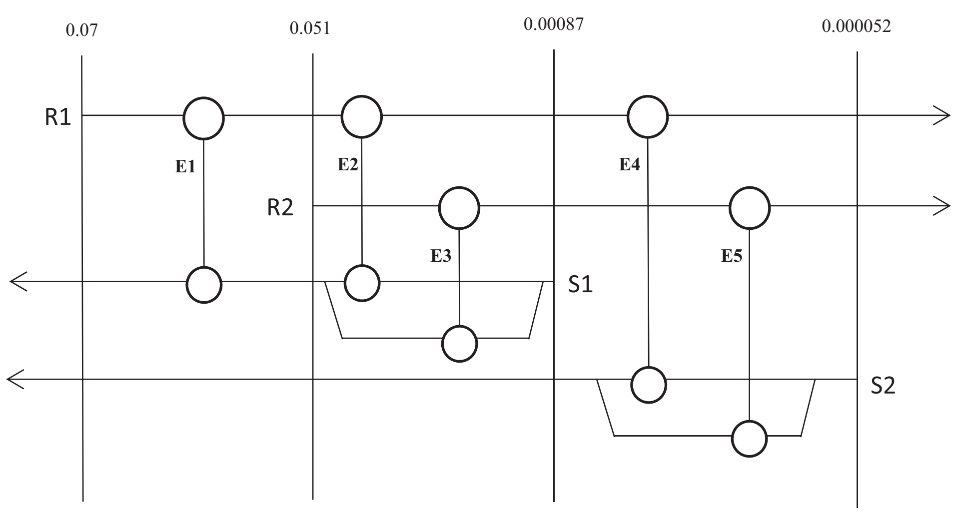

Fig. 5. Network topology for Example 1 for iterations 1–17 (Traditional solution).

Table 6
Detailed exchanger designs for the 5-exchanger solution in Example 1.

	E1	*E2*	*E3*	*E4*	*E5*
Packed Height (m)	1.543	4.532	1.391	2.369	1.460
Diameter (m)	0.729	0.725	0.418	0.664	0.321
Mass duty (kg/s)	0.04616	0.01597	0.004993	0.000583	9.65E-05
Rich flow (kg/s)	0.9	0.9	0.1	0.9	0.1
Lean flow (kg/s)	1.523	1.344	0.179	0.681	0.112
ky (kg/s/m^3)	0.049	0.049	0.026	0.045	0.032
Packing size (m)	0.036	0.036	0.021	0.033	0.016
Packing cost ($/m^3)	945.95	950.63	1423.27	1029.74	1610.17
ai (m^2/m^3)	127.91	128.57	219.55	140.156	285.10
Packing factor (m^{-1})	355.88	358.81	850.42	411.88	1282.12
Voidage	0.723	0.723	0.691	0.718	0.676
Pressure drop (kPa/m)	2.607	2.622	4.798	2.888	6.395

E stands for exchanger.

correction factors between runs 26 and 27. Fig. 7 shows how the 2 solutions converged between runs 26 and 27 such that the key parameters present in the MINLP converge to the values found in the detailed NLP solution. It also clearly shows how the MINLP was able to find a better solution at run 18 as a result of the multiple starts and the inclusion of correction factors. It is also possible to note, though perhaps difficult to see, that the TAC from iterations 18–27 actually marginally improve. This is not a result of vastly different solutions to the NLP, but rather due to the fact that small changes are made in the MINLP as a result of the updated correction factors included that guide the MINLP to slightly better values for the split flowrates and mass duties. Finally, by comparing the optimal rigorous solution (485,273$/y) with the traditional one obtained at iteration 1 (515,748$/y) it can be seen that about 6% of additional savings have been obtained due to the implementation of the proposed procedure with correction factors.

Table 8 shows the final values for the correction factors for each of the matches present. This table shows that it is difficult to predict the correct parameters in the MINLP without detailed knowledge of the problem beforehand, and that the degree to which they vary can be great, even when the same two streams are selected in different intervals. It also shows the large errors that can result from the simplified formulations used in traditional MINLP models when compared with more rigorous models.

5.2.2. Example 2

Example 2 consists of five rich streams and three lean streams, with the corresponding stream parameters shown in Tables 4 and 5. This example is among the largest MENS problem found in current MINLP literature and therefore serves to demonstrate the method's efficacy at producing effective networks for larger problems. This example, first presented by Hallale (1998), has also been solved by Szitkai et al. (2006), Emhamed et al. (2007), Isafiade and Fraser (2008) and Azeez et al. (2013). The initial values for the MINLP for Example 2 were $ai_{r,l,k} = 100$ m^2 m^{-3}, $ky_{r,l,k} = 0.05$ kg s^{-1} m^{-3}, $D_{r,l,k} = 0.5$ m, and $PackCost_{r,l,k} = 550\$\text{m}^{-3}$. Problem (MINLP) contains 845 equations, with 63 discrete variables and 813 continuous variables and Problem (NLP) contains 33,753 equations with 34,028 variables. Fig. 8 shows the solution that was obtained for the initial MINLP, which represents the solution that would be found if one were to use the "traditional" model and its variants. This solution, with 8 columns, gave a TAC of 298,863 $/y, but when a more detailed solution was found by the NLP, a TAC of 314,980$/y was found. The details and differences between the results for the first run are found in Table 9. This shows that, while the initial solution from the MINLP is good, it does not necessarily represent an achievable network in practice.

The algorithm was run for 100 iterations, generating many unique network configurations with which we found the network

Table 7
Detailed exchanger designs for the optimal solution for Example 1.

	E1	*E2*	*E3*	*E4*
Packed Height (m)	5.801	1.472	2.327	1.411
Diameter (m)	0.725	0.413	0.664	0.322
Mass duty (kg/s)	0.06214	0.000589	0.004995	9.46E-05
Rich flow (kg/s)	0.9	0.9	0.1	0.1
Lean flow (kg/s)	1.351	0.685	0.172	0.112
ky (kg/s/m^3)	0.049	0.026	0.045	0.032
Packing size (m)	0.036	0.021	0.033	0.016
Packing cost ($/m^3)	950.43	1431.93	1029.66	1609.17
ai (m^2/m^3)	128.54	222.02	140.14	284.67
Packing factor (m^{-1})	258.686	865.57	411.83	1279.07
Voidage	0.723	0.691	0.718	0.676
Pressure drop (kPa/m)	2.622	4.858	2.888	6.385

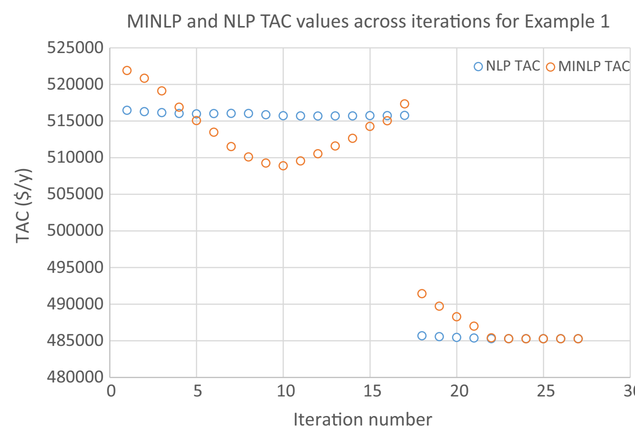

Fig. 7. Comparison of NLP TAC vs MINLP TAC across iterations for Example 1.

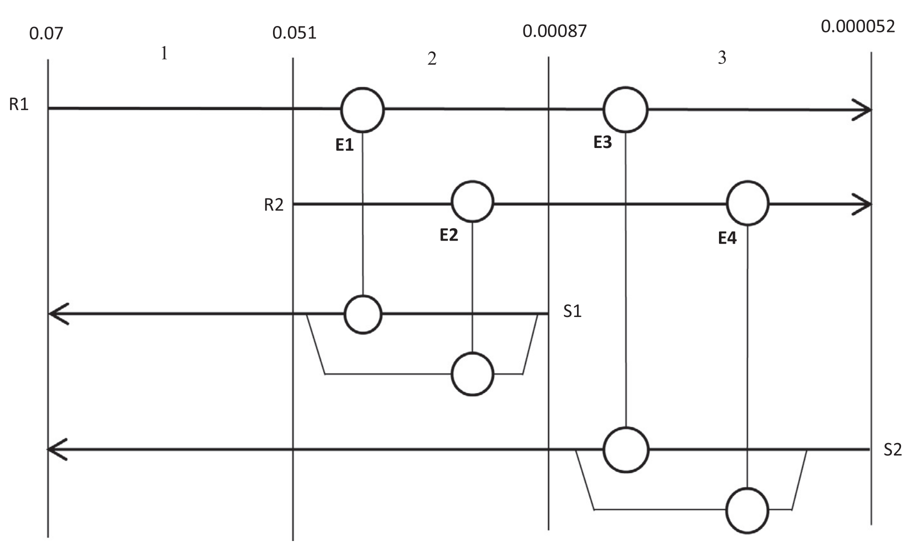

Fig. 6. Final network topology for Example 1.

Table 8
Final correction factors for Example 1.

Match	$Hcor_{r,l,k}$	$Dcor_{r,l,k}$	$kyCor_{r,l,k}$	$aiCor_{r,l,k}$	$PackCost_{r,l,k}$
1.1.1	1.02947	2.0829	0.98	0.4264	0.94596
1.1.2	0.68949	2.071	0.98	0.4285	0.95043
1.2.3	1.00556	1.897	0.9	0.4672	1.02967
2.1.2	0.77612	1.18	0.52	0.7401	1.43193
2.2.3	1.02446	0.92	0.64	0.9489	1.60917

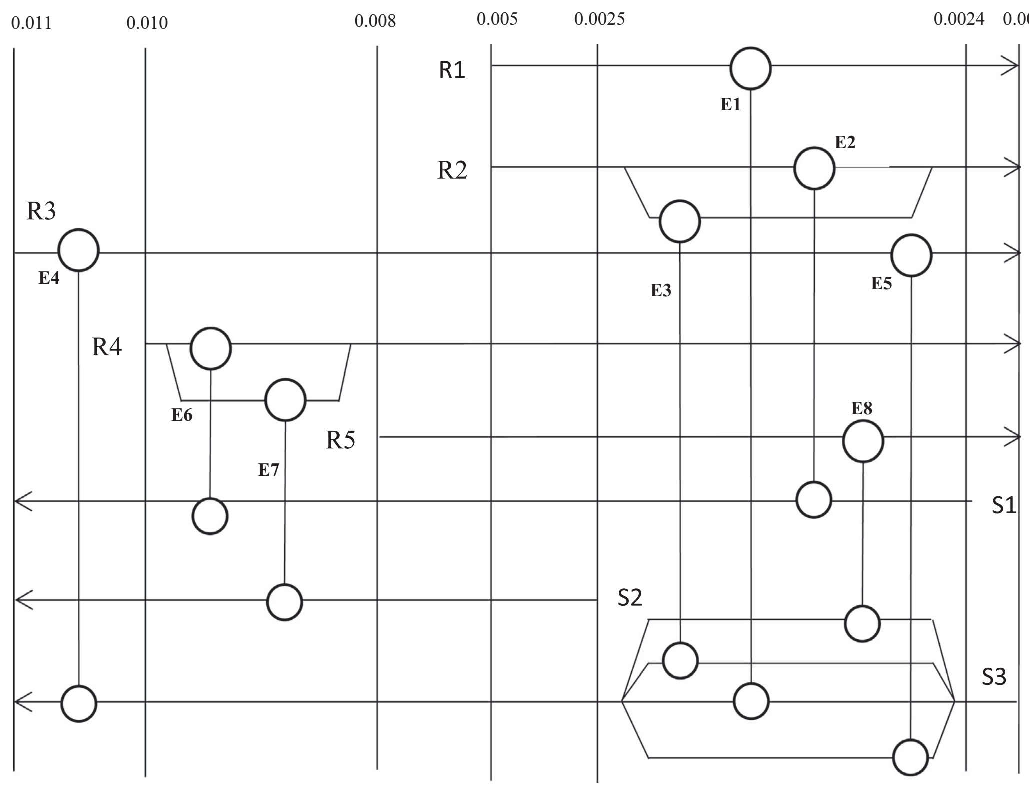

Fig. 8. Initial MINLP network topology for Example 2 (Traditional solution).

with the lowest TAC found by problem (NLP). This network was found at iteration 35 and contained 8 packed columns with a TAC of 307,349$/y which is about 2% improvement when compared to the traditional solution obtained without the implementation of the proposed procedure with correction factors. This detailed design is portrayed in Fig. 9, with the column designs shown in Table 10.

Note that the large differences between the fixed parameters in the MINLP and NLP solution are corrected through correction factors in the subsequent iterations. Fig. 10 shows the TAC values of the NLP and MINLP over the entire algorithm and Fig. 11 shows the relative differences. It is clear from these two figures that, as the algorithm progresses, the solutions for the networks more closely represent each other, with the final 10 iterations producing differences between the MINLP and NLP of less than 2% between iterations. While these solutions allow for the MINLP to select networks that can be created in reality, these solutions are not very close to the optimal solution.

The generation of so many different candidate networks is advantageous in searching for a global optimal network in such a large non-convex system. This is enabled by the multi-start procedure and the many different initial points provided by the shifting correction factors during each iteration. From Fig. 10 a number of the NLP TACs are very close to the best solution (iterations 4, 35, 49, and 91). Upon detailed analysis of these networks it can be found that these are 4 distinct networks with very close TACs, but differing topologies. This means that it is difficult for the MINLP solvers to find globally optimal solutions as multiple discrete variables give similar TACs.

Fig. 12 acts as a visual demonstration of the way in which correction factors change over the course of the algorithm. The long periods where the correction factor is unchanged is due to the fact that the specific match (i.e. 3, 3, 3) is not chosen during those iterations, or that there is no difference between the parameter in the MINLP and the correlating variable in the NLP. The figure shows the way in which the change to the correction factor is limited to not more than a 5% change between iterations. The full list of correction factors at the respective values at iteration 100 are included in Appendix C. An important question to raise here is why the MINLP generates such vastly different networks between certain iterations, despite the fact that the changes to the parameters are of such a small scale between the iterations. The reason for this is due, most likely, to the fact that many of the solutions generated by the MINLP are actually locally optimal.

Table 9
Initial solution network comparison of NLP to MINLP for Example 2.

	E1	*E2*	*E3*	*E4*	*E5*	*E6*	*E7*	*E8*
Mass duty (kg/s)	0.008	0.00338	0.00662	0.02036	0.00939	0.0051	0.0024	0.00275
Rich flow (kg/s)	1.791	1.309	1.432	5.543	1.945	1.3087	0.4	0.3759
Lean flow (kg/s)	2	1.79474	2.20526	3.5	3.5	1.1144	0.38563	0.5
Height (m):								
MINLP	4.306	2.0272	2.74	7.5111	3.463	1.8427	0.6921	0.7866
NLP	3.372	1.653	2.04	4.65	2.14	1.83	1.09	1.083
Diameter (m):								
MINLP	0.5	0.5	0.5	0.5	0.5	0.5	0.5	0.5
NLP	1.01	0.96	1.05	1.3	1.29	0.78	0.51	0.553
ky (kg/s/m^3):								
MINLP	0.05	0.05	0.05	0.05	0.05	0.05	0.05	0.05
NLP	0.048	0.048	0.048	0.046	0.046	0.049	0.047	0.05
Packing cost ($/m^3):								
MINLP	550	550	550	550	550	550	550	550
NLP	619.7	647.3	600.5	578.9	577.7	794.0	1167.3	1099.6
ai (m^2/m^3)								
MINLP	100	100	100	100	100	100	100	100
NLP	84.1	88.35	80.74	65.54	65.81	107.71	163.01	151.26
Packing size (m)	0.056	0.053	0.058	0.072	0.072	0.043	0.028	0.031
Pressure drop (kPa/m)	1.63	1.723	1.558	1.233	1.239	2.151	3.421	3.146

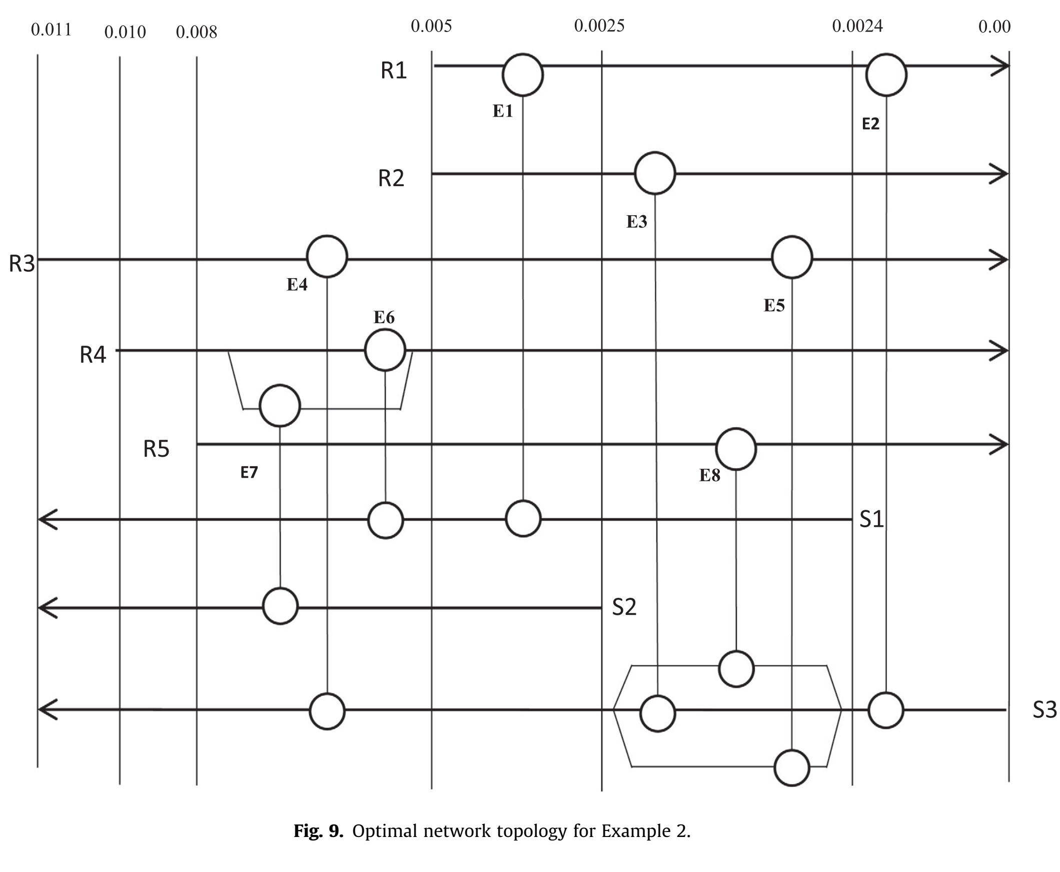

Fig. 9. Optimal network topology for Example 2.

It must be noted that the generation of the individual columns at the NLP level were found fairly quickly, with no iterations terminating due to infeasibilities. This demonstrates the robustness of the NLP formulation, as well as the abilities of CONOPT. However, this cannot be said of the MINLP. The solution procedure was interrupted numerous times, especially for Example 2, due to DICOPT's inability to find feasible solutions for the MINLP based on the new starting points provided by the changing correction factors. While it may be possible to use the "fairly linear" MINLP model of Szitkai et al. (2006) to allow for more robustness in the MINLP, it was decided to use a non-iso-compositional interval based superstructure model to avoid the exclusion of potential networks. The 'restarts' added substantially to the total time of solution for the method, as at each restart, new values for the value of M in the "big-M" constraint would help the solver to find feasible solutions.

Table 10
Optimal network column details for Example 2.

	E1	*E2*	*E3*	*E4*	*E5*	*E6*	*E7*	*E8*
Packed Height (m)	1.289	0.913	2.78	4.21	2.78	1.78	1.09	1.19
Diameter (m)	1.01	1.025	1.376	1.3	1.3	0.782	0.512	0.558
Mass duty (kg/s)	0.00327	0.00473	0.01	0.0196	0.01012	0.0051	0.0024	0.00275
ky (kg/s/m^3)	0.048	0.046	0.046	0.046	0.046	0.049	0.047	0.049
Packing size (m)	0.056	0.057	0.076	0.072	0.072	0.043	0.028	0.031
Packing cost ($/m^3)	620.86	611.03	602.7	578.91	577.90	794.24	1167.3	1091.9
ai (m^2/m^3)	84.3	82.65	61.99	65.536	65.77	107.74	163.00	149.99
Packing size (m)	0.056	0.057	0.076	0.072	0.072	0.043	0.028	0.031
Rich flow (kg/s)	1.2921	5.5561	2.6445	5.5561	2.46611	1.2921	0.4	0.4455
Lean flow (kg/s)	2	2	4	3.5	3.5	1.1143	0.3857	0.5
Pressure drop (kPa/m)	1.635	1.599	1.159	1.233	1.238	2.152	3.421	3.116

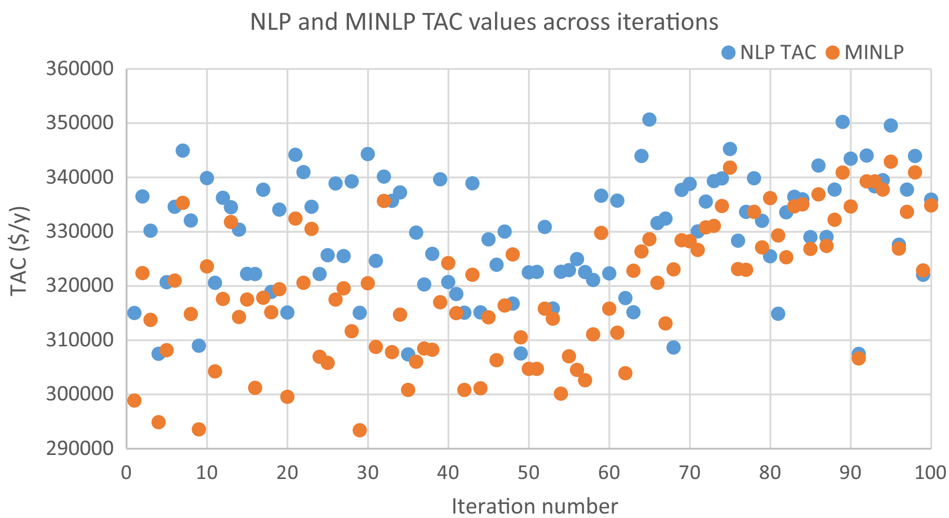

Fig. 10. Comparison of NLP solution to MINLP solution over the iterations.

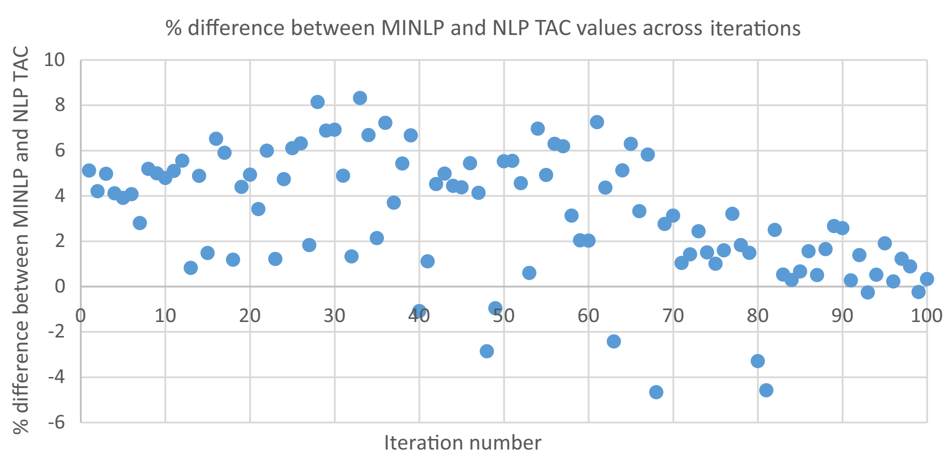

Fig. 11. Relative difference between NLP solutions to MINLP solutions over the iterations.

In both examples the column pressure drops set by the constraint in Eq. (33) were always active. This shows that the constraining factor in the selection of the packing size is the point at which flooding occurs. The inclusion of variable cost that includes the fact that smaller packing sizes are more expensive barely impacts the selection of smaller packing sizes. Meanwhile the trade-off between diameter and packing size is vitally important in the design of an optimally priced column. In previous methods the trade-off between the costs of internals, packing sizes, and diameters have not been considered, with other authors (Hallale & Fraser, 2000b; Isafiade & Short, 2016) using fixed packing parameters and subsequently changing these fixed parameters in the following run after flooding was considered in post processing. This study has presented a way to include these trade-offs implicitly in the network generation stage, while not adding further complexities associated with non-convexity into the MINLP. Moreover, we see that L/D constraints (Eqs. (19) and (20)) have little effect on the optimal solutions, as con-

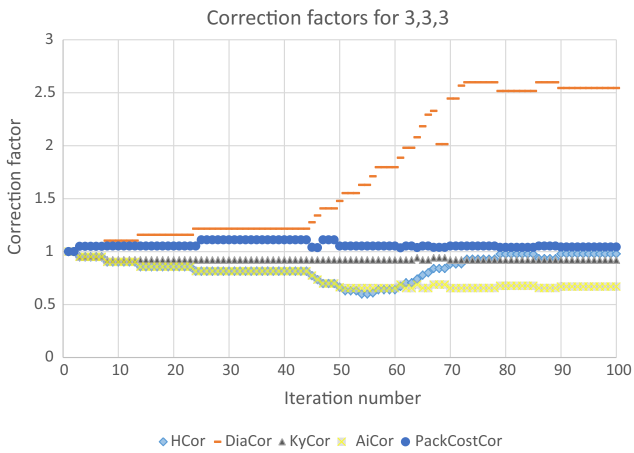

Fig. 12. Correction factors for a specific match (rich stream 3 with lean stream 3 in interval 3) over the iterations of the algorithm.

straints on packing size, diameter, and pressure drop are the actual limiting factors.

5. Conclusions

In this study detailed mass exchange network models were successfully designed and optimized using a novel combination of MINLP topology optimization based on shortcut models paired with a rigorous NLP individual unit optimization. This is a successful extension of the work of Short et al. (2016a), for heat exchanger network synthesis, to mass exchanger network synthesis. The novel two-step synthesis model allows for the use of relatively simple models in the network synthesis, with fewer non-convexities and more robust solutions. Nevertheless, it still accommodates details of the design that affect the capital costs from a rigorous NLP model, such as changes to the overall mass transfer coefficient, column diameters, costs associated with different sizes of packing, flooding considerations, and an overall height correction factor to account for reported discrepancies in the log mean composition difference approximation.

The model works by first deriving the network using an MINLP optimization method that utilizes shortcut models for the synthesis of the individual heat exchangers, with fixed mass transfer coefficients, packing costs, and column diameters, as well as using a log mean composition difference approximation, as has been done by other authors. The solution, with mass balances fixed, is then sent to an individual mass exchanger optimization that is modelled as an NLP utilizing a more rigorous approach including a differential equation that is converted into algebraic form using orthogonal collocation, common methods for determining the overall mass transfer coefficients, as well as newly developed equations for determining the optimal packing size based on flooding considerations and detailed costing functions. Once the optimal exchangers are found in this rigorous method, the shortcut models in the MINLP are updated with a series of correction factors. These correction factors are used to more accurately represent rigorous solutions in the shortcut models, while not increasing the level of non-linearity within the MINLP. The MINLP is then re-run and new designs obtained and the process repeated until the models converge to a solution where the NLP objective function is identical to the MINLP objective function, or until a maximum number of iterations is reached. During each iteration the current best solution, based on the total annual cost of the rigorously designed (NLP) network, is saved and compared, meaning that the converged solution does not necessarily have to be the optimal network. The correction factors are limited to a maximum of 5% change between iterations to ensure that potentially optimal solutions are not omitted.

Previous methods of MENS have reported great difficulty in finding feasible solutions, especially in large problems, even with the relatively simplified formulations used. In contrast, the proposed method allows for the MINLP model to remain simple, while still accounting for the intricacies involved in the design and optimization of mass exchanger columns using rigorous models. The rigorous NLP optimization in the outer loop gives realistic columns that can be used in a real plant scenario, whereas the models of many other authors have given designs that have not been verified and were often unrealistic in size and therefore not suitable for industrial application. Furthermore, the solutions of the two case studies demonstrated the additional saving of 6% and 2% when compared to the traditional solutions. Therefore, notably savings can be expected when applying the proposed iterative procedure with correction factors.

While the novel method does not guarantee globally optimal solutions, multiple iterations with a variety of starting conditions from correction factors means indicate a greater likelihood at finding the global optimum. This has been demonstrated in the examples, where new topologies were found after a number of iterations that gave superior total annual costs.

Further work is planned on applying the principles derived in this work with different NLP column optimization methods, water networks, and combined mass and heat exchanger networks that can include rigorous thermodynamic models for the heat and mass transfer coefficients along the column. A possibility of merging rich streams in the MEN superstructure in order to obtain solution with fewer columns could also be investigated.

Acknowledgements

This study is supported by the National Research Foundation of South Africa (Grant numbers: 85536 and 87744), the Visiting Scholar Fund of the Research Office of the University of Cape Town, South Africa, and the Slovenian Research Agency's Program P2-0032 and project L2-7633. The funds are gratefully acknowledged.

Appendix A. MINLP model equations

The MINLP is modelled in similar fashion to the existing MENS MINLP models discussed in the body of the paper. The basis for the model is that of Azeez et al. (2013), with an updated objective function, as well as the additional Eqs. (1)(6) that ensure that iso-compositional mixing is not enforced. These equations and the explanation are found in the main body of the study. In this formulation, the superstructure is defined by the supply compositions of the rich and lean streams, as illustrated in Fig. 1. The following paragraphs show the equations used in the MINLP optimization section of this study.

If we use Fig. 1 as an illustrative example, the following equations will represent the superstructure in the model; where the compositions are sorted so that the highest supply composition is on the left of the superstructure and compositions monotonically decrease towards the right:

$$\begin{aligned}
k=1: &\quad Y^{s}_{R1}=y_{R1,1};\quad Y^{*t}_{S1}=y^{*}_{S1,1};\quad Y^{*t}_{S2}=y^{*}_{S2,1}\\
k=2: &\quad Y^{s}_{R2}=y_{R2,2}\\
k=3: &\quad Y^{*s}_{S2}=y^{*}_{S2,3}\\
k=4: &\quad Y^{*s}_{S1}=y^{*}_{S1,4};\quad Y^{t}_{R1}=y_{R1,4};\quad Y^{t}_{R2}=y_{R2,4}
\end{aligned}\tag{A1}$$

Eqs. (A2) and (A3) ensure that compositions decrease monotonically along the superstructure.

$$y_{r,k} \geqslant y_{r,k+1} \qquad k \in K, r \in R \tag{A2}$$

$$y^*_{l,k} \geqslant y^*_{l,k+1} \qquad k \in K,\ l \in S, \tag{A3}$$

Eqs. (A4) and (A5) represent the overall mass balances for all streams across all of the intervals. These equations guarantee that the target compositions are met.

$$(Y^s_r - Y^t_r)G_r = \sum_{k \in K}\sum_{l \in S} M_{r,l,k} \qquad r \in R \tag{A4}$$

$$(Y^{*t}_l - Y^{*s}_l)L_l = \sum_{k \in K}\sum_{r \in R} M_{r,l,k} \qquad l \in S \tag{A5}$$

where the supply and target compositions of the rich streams are represented by Y^s_r and Y^t_r respectively, while the supply and target compositions of the lean streams are represented by Y^{*t}_l and Y^{*s}_l respectively. $M_{r,l,k}$ is the amount of mass exchanged between the rich stream, r, and lean stream, l, in interval, k. G_r and L_l are the flowrates of the respective rich and lean streams.

Similarly to Eqs. (A4) and (A5), each rich and lean stream requires a mass balance over each interval of the superstructure. Eqs. (A6) and (A7), below, represent the rich and lean streams respectively.

$$(y_{r,k} - y_{r,k+1})G_r = \sum_{l \in S} M_{r,l,k} \qquad r \in R,\ k \in K \tag{A6}$$

$$(y^*_{l,k} - y^*_{l,k+1})L_l = \sum_{r \in R} M_{r,l,k} \qquad l \in S,\ k \in K \tag{A7}$$

where the intermediate compositions of rich streams are represented by $y_{r,k}$ and those of the lean streams by $y^*_{l,k}$. In order to ensure numerical stability Big-M constraints (Eq. (A8)) are included that force the mass exchanged in an exchanger to zero when the binary variable $z_{r,l,k}$ takes a zero value (Szitkai et al., 2006).

$$M_{r,l,k} - \Omega_{r,l} z_{r,l,k} \leqslant 0 \qquad r \in R,\ l \in S,\ k \in K \tag{A8}$$

where the scalar $\Omega_{r,l}$ is an upper bound on the amount of mass that can be exchanged between the two streams in question. Eqs. (A9) and (A10) are utilized to calculate the driving forces at the ends of each packed column, represented by $dy_{r,l,k}$.

$$dy_{r,l,k} \leqslant y_{r,k} - y^*_{l,k+1} + \Phi_{r,l}(1 - z_{r,l,k}) \qquad k \in K,\ r \in R,\ l \in S \tag{A9}$$

$$dyrl_{r,l,k} \leqslant yr_{r,l,k} - yl^*_{r,l,k} + \Phi_{r,l}(1 - z_{r,l,k}) \qquad k \in K,\ r \in R,\ l \in S \tag{A10}$$

In a similar formulation to (A8), when a binary variable has a value of '1' then the driving force, $dy_{r,l,k}$, is calculated. In order to avoid the possibility of negative driving forces, the parameter $\Phi_{r,l}$ is included. This parameter represents the upper bound of the driving force and is calculated from the problem-specific stream data.

Due to the presence of logarithms in the actual LMCD equation singularities may form, resulting in solver failure. In order to circumvent these issues, various approximations have been posited. A review of the various approximations is available in Shenoy and Fraser (2003). This study makes use of the most common approximation, that of Chen (1987) (A11).

$$LMCD_{r,l,k} = \left[\frac{(dy_{r,l,k})(dyrl_{r,l,k})(dy_{r,l,k} + dyrl_{r,l,k})}{2}\right]^{\frac{1}{3}} \tag{A11}$$

The height of each column (or exchanger) is calculated using Eq. (A12). Note that in this equation, the LMCD is approximated and the mass transfer coefficient, $kya_{r,l,k}$, column diameter, $D_{r,l,k}$, and column diameter correction factor, $Dcor_{r,l,k}$, are not variables in the MINLP optimization and are thus fixed during each successive MINLP run.

$$H_{r,l,k} = \frac{M_{r,l,k}}{kya_{r,l,k} \cdot \frac{\pi}{4}(Dcor_{r,l,k} \cdot D_{r,l,k})^2 \times LMCD_{r,l,k}} \tag{A12}$$

It should be noted that $kya_{r,l,k}$ is the mass transfer coefficient multiplied by the interfacial area, described by Eq. (2) in the main body of the paper and that the diameter is modified by a correction factor, with the details of its use described fully in the main body of the paper.

Eqs. (A1)–(A12), combined with Eqs. (1)–(6), presented in the body of the text, represent the full MINLP model that is utilized in the paper. The implementation of this MINLP with the NLP sub-optimization is detailed in the main paper.

Appendix B. Packing characteristics equations

As mentioned in the main body of the paper, the packing characteristics are needed in the NLP section of the model in order to allow for an optimal packing size to be selected. The packing characteristics are taken from standard tables found in Perry's Chemical Engineering Handbook (Green and Perry, 2008) and fitted to curves. The Figs. B1–B5 show the curves, as well as the equations used in the model with their R^2 values. While the fits are in no way ideal, the authors feel that they are within a good enough tolerance for the purposes of the model. The tables below are for carbon steel Raschig rings, as done by other authors for the example studied. The costing, seen in Fig. B4, has been updated from the original date of 1990 to 2000 in order to compare with the date of the other costing functions used by other authors.

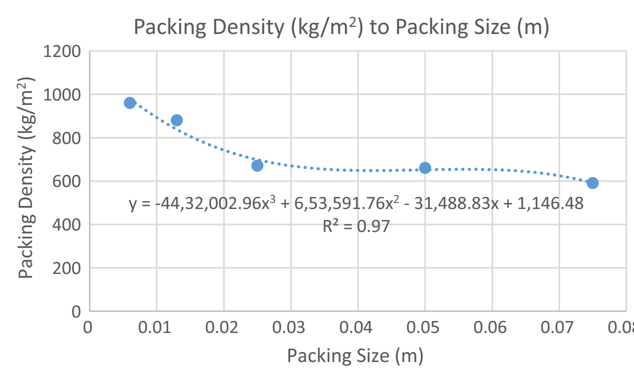

Fig. B1. Curve fit of data from Perry's Chemical Engineering Handbook (Green and Perry, 2008) for Packing Density versus Packing Size.

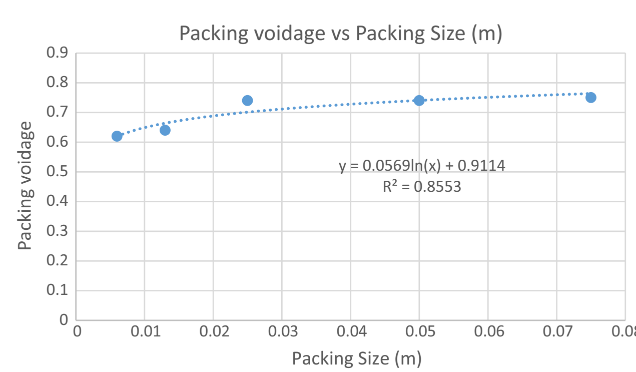

Fig. B2. Curve fit of data from Perry's Chemical Engineering Handbook (Green and Perry, 2008) for Packing voidage versus Packing Size.

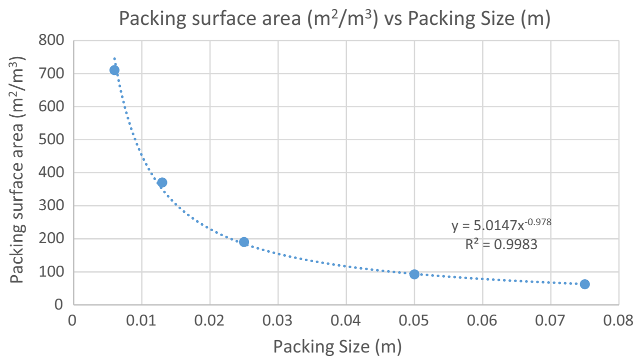

Fig. B3. Curve fit of data from Perry's Chemical Engineering Handbook (Green and Perry, 2008) for Packing surface area versus Packing Size.

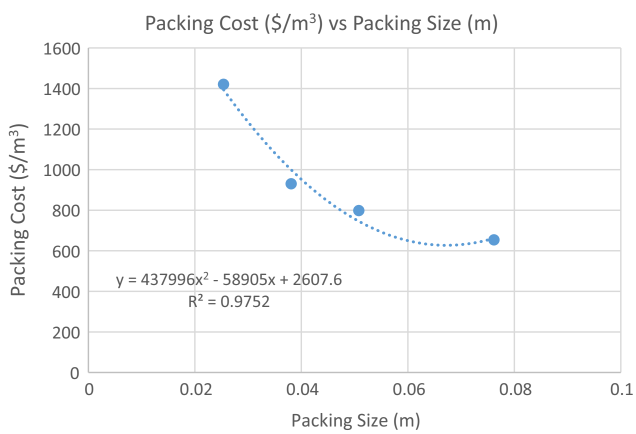

Fig. B4. Curve fit of data from Perry's Chemical Engineering Handbook (Green and Perry, 2008) for Packing costing vs Packing Size.

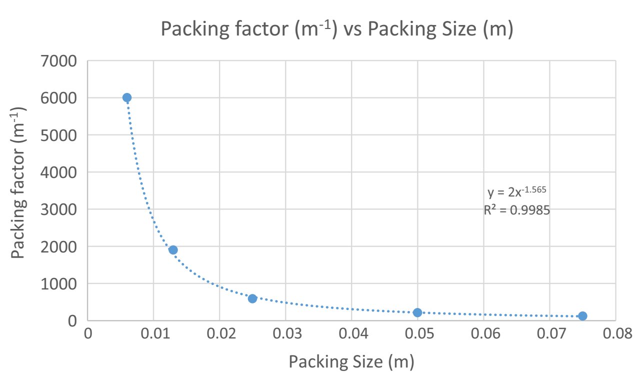

Fig. B5. Curve fit of data from Perry's Chemical Engineering Handbook (Green and Perry, 2008) for Packing factor vs Packing size.

Appendix C. Final correction factors for Example 2

This appendix contains the final values for the correction factors used in Example 2 (i.e. at iteration 100). A value of 1 means that the match was not selected at any point during the algorithm. It is shown as it gives the reader an idea of the varying and unpredictable nature of the corrections that are required and how the simplified equations in standard MINLP methods are not able to accurately predict the actual sizes and internals of packed columns without access to more detailed equations (see Table C1).

Table C1
Values for the correction factors at iteration 100 for Example 2.

	HeightCor	*DiaCor*	*KyCor*	*AiCor*	*PackCostCor*
1.1.4	1.07782	1.795856	0.96	0.8422	1.1280
1.1.5	1.02659	1.710339	0.96	0.8429	1.1287
1.1.6	1	1	1	1	1
1.2.4	1.20728	2.002	0.96	0.8461	1.1323
1.2.5	1	1	1	1	1
1.2.6	1	1	1	1	1
1.3.4	0.95	1.05	0.95	0.95	1.05
1.3.5	1.2224	2.016	0.96	0.8407	1.1263
1.3.6	1.2732	2.014	0.96	0.8413	1.1270
2.1.4	0.9429	1.4071	0.94	0.9841	1.2181
2.1.5	0.86266	2.734679	0.92	0.6205	1.0949
2.1.6	1	1	1	1	1
2.2.4	1.03954	1.269908	0.893	0.9405	1.333
2.2.5	1	1	1	1	1
2.2.6	1	1	1	1	1
2.3.4	0.9878	2.5809	0.92	0.6579	1.0872
2.3.5	0.96263	2.724583	0.92	0.6198	1.0960
2.3.6	0.89423	2.75	0.92	0.62037	1.0951
3.1.1	0.80162	1.4071	0.92	0.6983	1.0501
3.1.2	1.54745	1.314	0.96	1.2766	1.5515
3.1.3	1.21551	1.106	0.98	1.2155	1.2155
3.1.4	1.05	1.05	0.98	1.05	1.05
3.1.5	1.05	1.05	0.98	1.05	1.05
3.1.6	1	1	1	1	1
3.2.1	0.98042	2.584	0.92	0.6591	1.0450
3.2.2	1.04738	0.954	0.85738	1.0474	1.1573
3.2.3	1.21551	0.966	0.81451	1.2155	1.2155
3.2.4	0.9025	1.1025	0.92	0.9025	1.0497
3.2.5	1	1	1	1	1
3.2.6	1	1	1	1	1
3.3.1	0.9580	2.6	0.92	0.6554	1.0525
3.3.2	1.06677	2.342	0.94	0.7256	1.0380
3.3.3	0.97872	2.544	0.92	0.6696	1.0430
3.3.4	1.02784	2.4624	0.94	0.6904	1.0450
3.3.5	0.9798	2.59	0.92	0.6576	1.0508
3.3.6	0.95306	2.588	0.92	0.6582	1.0503
4.1.2	1.6094	1.568	0.98	1.0752	1.4410
4.1.3	1.42269	1.748818	0.96	0.9522	1.2675
4.1.4	0.95	1.05	0.98	0.9588	1.05
4.1.5	1	1	1	1	1
4.1.6	1	1	1	1	1
4.2.2	2.43829	1.0469	0.94	1.5939	2.1055
4.2.3	2.10936	1.088537	0.9	1.5207	2.006
4.2.4	0.95	1.05	0.98	0.9613	1.05
4.2.5	1	1	1	1	1
4.2.6	1	1	1	1	1
4.3.2	1.41224	1.782	0.96	0.9480	1.2619
4.3.3	0.97723	1.276282	0.912	0.92996	1.2173
4.3.4	1	1	1	1	1
4.3.5	1	1	1	1	1
4.3.6	1	1	1	1	1
5.1.3	1.97993	1.1613	0.95	1.4364	1.8796
5.1.4	1.21551	1.1802	0.90024	1.2155	1.2155
5.1.5	1.6289	1.216	0.84	1.3769	1.6289
5.1.6	1	1	1	1	1
5.2.3	2.1829	1.108	0.987	1.5081	1.9943
5.2.4	1.1576	1.1576	0.92	1.1576	1.1576
5.2.5	1	1	1	1	1
5.2.6	1	1	1	1	1
5.3.3	1.1576	1.142	0.94	1.1576	1.1576
5.3.4	1.88565	1.116	0.98	1.4984	1.8856
5.3.5	2.48975	1.1718	0.931	1.4248	1.8859
5.3.6	2.29915	1.106	1	1.5131	1.9997

References

Azeez, O.S., Isafiade, A.J., Fraser, D.M., 2012. Supply and target based superstructure synthesis of heat and mass exchanger networks. Chem. Eng. Res. Des. 90 (July), 266–287.

Azeez, O.S., Isafiade, A.J., Fraser, D.M., 2013. Supply-based superstructure synthesis of heat and mass exchange networks. Comput. Chem. Eng. 56, 184–201.

Biegler, L.T., 2007. An overview of simultaneous strategies for dynamic optimization. Chem. Eng. Process. 46, 1043–1053.

Biegler, L.T., Logsdon, J.S., 1989. Accurate solution of differential-algebraic optimisation problems. Ind. Eng. Chem. Res. 28, 1628–1639.

Chen, J.J.J., 1987. Letter to the editor: comments on the improvements on a replacement for the logarithmic mean. Chem. Eng. Sci. 42, 2488–2489.

Ciric, A.R., Floudas, C.A., 1989. A retrofit approach for heat exchanger networks. Comput. Chem. Eng. 13 (6), 703–715.

Comeaux, R.G., 2000. Synthesis of MENs with Minimum Total Cost. UMIST, Manchester (MPhil).

Douglas, J.M., 1988. Conceptual Design of Chemical Processes. McGraw-Hill, New York.

El-Halwagi, M.M., Manousiouthakis, V., 1989. Synthesis of mass exchange networks. AICHE J. 35 (8), 1233–1244.

El-Halwagi, M.M., Manousiouthakis, V., 1990a. Automatic synthesis of mass-exchange networks with single-component targets. Chem. Eng. Sci. 45 (9), 2813–2831.

El-Halwagi, M.M., Manousiouthakis, V., 1990b. Simultaneous synthesis of mass-exchange and regeneration networks. AIChE J. 36 (8), 1209–1219.

El-Halwagi, M.M., 1997. Pollution Prevention through Process Integration: Systematic Design Tools. Academic Press, San Diego, USA.

Emhamed, A.M., Lelkes, Z., Rev, E., Farkas, T., Fonyo, Z., Fraser, D.M., 2007. New hybrid method for mass exchange network optimization. Chem. Eng. Commun. 194 (12), 1688–1701.

Green, D.W., Perry, R.H., 2008, Perry's Chemical Engineers' Handbook, eighth ed. McGraw-Hill (Chaper 14)

Hallale, N., 1998. Capital Cost Targets for the Optimum Synthesis of Mass Exchange Networks (Ph.D. thesis). Department of Chemical Engineering, University of Cape Town.

Hallale, N., Fraser, D.M., 2000a. Capital and total cost targets for mass exchange networks part 1: Simple capital cost models. Comput. Chem. Eng. 23, 1661–1679.

Hallale, N., Fraser, D.M., 2000b. Capital and total cost targets for mass exchange networks part 2: Detailed capital cost models. Comput. Chem. Eng. 23, 1681–1699.

Hallale, N., Fraser, D.M., 2000c. Supertargeting for mass exchange networks Part I: Targeting and design techniques. Chem. Eng. Res. Design 78 (A2), 202–207.

Ibrahim, H.A-H., 2014. In: Bennet, Kelly (Ed.), Design of Fractionation Columns, MATLAB Applications for the Practical Engineer. InTech. 10.5772/57249. Available from: <http://www.intechopen.com/books/matlab-applications-for-the-practical-engineer/design-of-fractionation-columns>.

Isafiade, A.J., Fraser, D.M., 2008. Interval based MINLP superstructure synthesis of mass exchanger networks. Chem. Eng. Res. Des. 86 (8), 909–924.

Isafiade, A.J., Short, M., 2016. Synthesis of mass exchange networks for single and multiple periods of operations considering detailed cost functions and column performance. Process Saf. Environ. Prot. 103, 377–390.

Jamialahmadi, M., Muller-Steinhagen, H., Izadpanah, M.R., 2005. Pressure drop, gas hold-up and heat transfer during single and two-phase flow through porous media. Int. J. Heat Fluid Flow 26, 156–172.

Karacan, S., Cabbar, Y., Alpbaz, M., Hapoglu, H., 1998. The steady-state and dynamic analysis of packed distillation column based on partial differential approach. Chem. Eng. Process. 37, 379–388.

Kister, H.Z., Gill, D.R., 1991. Predict flood point and pressure-drop for modern random packings. Chem. Eng. Prog. 87 (2), 32–42.

Leva, M., 1953. Tower Packings and Packed Tower Design. The United States Stoneware Company, Akron, USA.

Liu, L., Du, J., El-Halwagi, M.M., Ponce-Ortega, J.M., Yao, P., 2013. Synthesis of multi-component mass-exchange networks. Chin. J. Chem. Eng. 21 (4), 376–381.

Mores, P., Scenna, N., Mussati, S., 2012. A rate based model of a packed column for CO_2 absorption using aqueous monoethanolamine solution. Int. J. Greenhouse Gas Control 6, 21–36.

Onda, K., Takeuchi, H., Okumoto, Y., 1968. Mass transfer coefficients between gas and liquid phases in packed columns. J. Chem. Eng. Jpn. 1, 56–61.

Papalexandri, K.P., Pistikopoulos, E.N., Floudas, C.A., 1994. Mass exchange networks for waste minimisation: a simultaneous approach. Trans. IChemE, Part A 72, 279–294.

Shenoy, U.V., Fraser, D.M., 2003. A new formulation of the Kremser equation for sizing mass exchangers. Chem Eng. Sci. 58, 5121–5124.

Short, M., Isafiade, A.J., Fraser, D.M., Kravanja, Z., 2016a. Synthesis of heat exchanger networks using mathematical programming and heuristics in a two-step optimisation procedure with detailed exchanger design. Chem. Eng. Sci. 144, 372–385.

Short, M., Isafiade, A.J., Fraser, D.M., Kravanja, Z., 2016b. Two-step hybrid approach for the synthesis of multi-period heat exchanger networks with detailed exchanger design. Appl. Therm. Eng. 105, 807–821.

Sinnot, R.K., 2005. Chemical Engineering Design, vol. 6. Butterworth-Heinemann, Oxford, UK.

Szitkai, Z., Farkas, T., Lelkes, Z., Rev, E., Fonyo, Z., Kravanja, Z., 2006. Fairly linear mixed integer nonlinear programming model for the synthesis of mass exchange networks. Ind. Eng. Chem. Res. 45, 236–244.

Yee, T.F., Grossmann, I.E., 1990. Simultaneous optimization models for heat integration-II. Heat exchanger network synthesis. Comp. Chem. Eng. 14 (10), 1165–1184.